

Non-sterile electroweak-scale right-handed neutrinos and the dual nature of the 126-GeV scalar

Vinh Hoang,^{1,*} Pham Q. Hung,^{1,2,†} and Ajinkya Shrish Kamat^{1,‡}

¹*Department of Physics, University of Virginia, Charlottesville, VA 22904-4714, USA*

²*Center for Theoretical and Computational Physics, Hue University College of Education, Hue, Vietnam*

(Dated: April 21, 2022)

Can, and under which conditions, the 126-GeV SM-like scalar with the signal strengths for its decays into W^+W^- , ZZ , $\gamma\gamma$, $b\bar{b}$ and $\tau\bar{\tau}$ being consistent with the SM predictions be accommodated in models that go beyond the Standard Model? Is it truly what it appears to be? A minimal extension of the original electroweak-scale right-handed neutrino model, in which right-handed neutrinos naturally obtain electroweak-scale masses, shows a scalar spectrum which includes the 126-GeV SM-like scalar possessing signal strengths compatible with experiment but also a dual nature quite unlike that of the Standard Model. In other words, the 126-GeV SM-like scalar could be an *impostor*.

I. INTRODUCTION

The discovery of the 126-GeV SM-like scalar [1] and the present absence of any new physics signals has opened up a whole host of questions as to the true nature of the electroweak symmetry breaking and to what may lie beyond the Standard Model. The sole existence of the 126-GeV particle would leave unanswered several deep questions such as the origin of neutrino masses, the hierarchy of quark and lepton masses among many others. It also implies that the electroweak vacuum is metastable with drastic consequences in the very far-distant future [2]. It remains to be seen whether this most simple picture- albeit one with many question marks- will be the ultimate theory of nature or it is merely an effective theory at current accessible energies whose reality tests are incomplete and more non-SM phenomena will pop up in the not-too-distant future with Run II of the LHC.

Despite the present lack of new physics at the LHC, it does not imply that it is not there. On the contrary, new physics has already appeared in the neutrino sector through neutrino oscillation and its implication on neutrino masses. This evidence, although quite clear, is only indirect and does not show where the new physics that gives rise to the aforementioned phenomena may appear. This difficulty in finding a direct evidence for the new physics involved in generating neutrino masses is compounded by the fact that these masses are so tiny, more than seven orders of magnitude smaller than the light-

est lepton: the electron. In the most generic scenario of the elegant seesaw mechanism for generating tiny masses, the right-handed neutrinos are sterile i.e. singlets under the electroweak gauge group. In a nutshell, the two mass eigenvalues are m_D^2/M and M where the Dirac mass m_D is proportional to the electroweak scale while the Majorana mass M is $\gg m_D$. In addition to the fact that ν_R 's are assumed to be electroweak singlets, the very large values for M in a generic scenario makes it very very difficult to probe the crucial physics, namely that which gives rise to M which is responsible for the lightness of the “active” neutrinos. Another facet of this new physics is the Majorana nature of the “active” neutrinos themselves which could manifest itself through neutrino less double beta decays which so far have not been observed. Through neutrino oscillations, we have a hint of new physics but what it might be and where to look for it is still a big mystery at the present time.

The aforementioned uncertainties rest in large part on the assumption that right-handed neutrinos are electroweak singlets. This usually comes from a certain extension of the SM such as the Left-Right symmetric model $SU(2)_L \times SU(2)_R \times U(1)_{B-L}$ [3] or the Grand Unified model $SO(10)$, among others. It goes without saying that the singlet assumption is not verified in the absence of experimental signals of right-handed neutrinos. If one is however willing to entertain the idea that right-handed neutrinos *are not* sterile, there is an entire panorama of accessible phenomena that can be searched for and studied. A non-sterile right-handed neutrino necessarily interacts with the electroweak gauge bosons and the Majorana mass term is expected to carry the electroweak quantum number and hence is proportional to

* vvh9ux@virginia.edu

† pqh@virginia.edu

‡ ask4db@virginia.edu

the electroweak breaking scale. Right-handed neutrinos could then be searched for both from an interaction point of view and from an energetic one. A model of this kind was put forth by one of us (PQH) [4] (the $EW\nu_R$ model).

In the $EW\nu_R$ model [4], right-handed neutrinos are parts of $SU(2)$ doublets along with their charged partners (the mirror charged leptons). Anomaly freedom dictates the existence of doublets of right-handed mirror quarks. The particle content of the model is listed in the next section. The existence of extra doublets of chiral fermions, the mirror quarks and leptons, is potentially fatal for the model because of their contributions to the electroweak precision parameters, in particular the S-parameter. Those extra chiral doublets would make a “large” contribution to the S-parameter, an undesirable outcome. Fortunately, the $EW\nu_R$ model contains a Higgs triplet which makes opposite contributions to the S-parameter and thus offsetting those of the mirror fermions. An exhaustive study of the electroweak precision parameters within the framework of the $EW\nu_R$ model has been carried out in [6] with the main result being that there is a large parameter space which satisfies the precision constraints.

The $EW\nu_R$ model in its original inception [4] contains, beside one Higgs doublet which couples to both SM and mirror fermions, two scalar triplets, one (complex) with hypercharge $Y/2 = 1$ and another (real) with $Y/2 = 0$. Out of the thirteen degrees of freedom (4 for the doublet, 6 for the complex triplet and 3 for the real triplet), three are absorbed by W 's and Z and the remaining *ten* become physical degrees of freedom. Can one of those ten physical scalars describe the observed 126-GeV SM-like scalar? If not, what minimal extension would be needed for that purpose? Where and how does one look for the more massive scalars which could be CP even or odd?

The plan of the paper is as follows. Section II will be devoted to a summary of the $EW\nu_R$ model with its particle content and, in particular for this paper, its scalar sector. For completeness, the electroweak precision parameter constraints will also be summarized. Section III presents some of the salient points concerning the scalar sector of the original $EW\nu_R$ model. A particular attention is paid to what this sector has to say about the 126-GeV SM-like scalar. We show why the lightest spin-0 particle has to be CP-odd if one wishes to identify it with the 126-GeV object. This has to do with the fact that the production cross section for the scalar is very large compared with the equivalent SM quantity. This

occurs when a single Higgs doublet couples to both SM and mirror fermions. The CP-odd option unfortunately is ruled out by the likelihood analysis which favors the CP-even case [7]. At the end of this section we present a simple extension of the original model by adding one extra Higgs doublet. In this extension, by imposing a global symmetry, one Higgs doublet is made to couple to SM fermions while the other one couples only to mirror fermions. The scalar mass eigenstates and eigenvalues are shown as well as their couplings to fermions and gauge bosons. Section IV discusses the implications of the extended model in light of the existence of the 126-GeV SM-like scalar. We will show in that section the dual nature of the 126-GeV SM-like scalar and only further measurements can tell whether or not it is an “impostor”.

II. THE $EW\nu_R$ MODEL: A SUMMARY

The main idea of the $EW\nu_R$ model [4] was to search for a model in which right-handed neutrinos *naturally* acquire a mass proportional to the electroweak scale $\Lambda_{EW} = 246$ GeV. For this to occur, the *most natural* way to implement this idea is for right-handed neutrinos to be *non-sterile*. In particular, the simplest way is to put them in doublets along with right-handed mirror charged lepton partners. In this manner, a Majorana mass term of the type $M\nu_R^T\sigma_2\nu_R$ necessarily carries an $SU(2)\times U(1)$ quantum number and transforms like an $SU(2)$ triplet. (Details are summarized below.) As shown in [4], a new Higgs sector including triplets is needed and it obviously participates in the symmetry breaking of the electroweak gauge group. The $EW\nu_R$ model of [4] is highly testable for the following reasons: 1) ν_R 's are sufficiently light; 2) ν_R 's couple to W and Z and can be produced through these couplings; 3) The presence of an extended Higgs sector.

A. Gauge structure and particle content of the $EW\nu_R$ model

Below is a summary of the gauge structure and particle content of the minimal $EW\nu_R$ model of [4]. The notations for the leptons and quarks are generic for any family.

- Gauge group: $SU(3)_C \times SU(2) \times U(1)_Y$
- Lepton $SU(2)$ doublets (generic notation):

SM:

$$l_L = \begin{pmatrix} \nu_L \\ e_L \end{pmatrix}; \quad (1)$$

Mirror:

$$l_R^M = \begin{pmatrix} \nu_R \\ e_R^M \end{pmatrix}. \quad (2)$$

- Lepton $SU(2)$ singlets (generic notation):

SM: e_R ; Mirror: e_L^M

- Quark $SU(2)$ doublets (generic notation):

SM:

$$q_L = \begin{pmatrix} u_L \\ d_L \end{pmatrix}; \quad (3)$$

Mirror:

$$q_R^M = \begin{pmatrix} u_R^M \\ d_R^M \end{pmatrix}. \quad (4)$$

- Quark $SU(2)$ singlets (generic notation):

SM: u_R, d_R ; Mirror: u_L^M, d_L^M .

- The Higgs sector:

a) One Higgs doublet: Φ . This Higgs doublet couples to both SM and mirror fermions.

b) One complex Higgs triplet with $Y/2 = 1$ containing doubly-charged scalars:

$$\tilde{\chi} = \frac{1}{\sqrt{2}} \vec{\tau} \cdot \vec{\chi} = \begin{pmatrix} \frac{1}{\sqrt{2}} \chi^+ & \chi^{++} \\ \chi^0 & -\frac{1}{\sqrt{2}} \chi^+ \end{pmatrix}. \quad (5)$$

c) One real Higgs triplet with $Y/2 = 0$:

$$(\xi^+, \xi^0, \xi^-). \quad (6)$$

d) One SM singlet Higgs: ϕ_S .

B. Symmetry breaking in the $EW\nu_R$ model

$SU(2) \times U(1)$ is spontaneously broken by the vacuum expectation values (VEV) of the Higgs doublet and triplets. The Higgs potential [4, 17] has a global $SU(2)_L \times SU(2)_R$ symmetry. The triplets transform as

$(3, 3)$ and the doublet as $(2, 2)$ under that global symmetry. Specifically,

$$\chi = \begin{pmatrix} \chi^0 & \xi^+ & \chi^{++} \\ \chi^- & \xi^0 & \chi^+ \\ \chi^{--} & \xi^- & \chi^{0*} \end{pmatrix}, \quad (7)$$

and

$$\Phi = \begin{pmatrix} \phi^0 & \phi^+ \\ \phi^- & \phi^0 \end{pmatrix}. \quad (8)$$

Proper vacuum alignment dictates $\langle \chi^0 \rangle = \langle \xi^0 \rangle = v_M$ i.e.

$$\langle \chi \rangle = \begin{pmatrix} v_M & 0 & 0 \\ 0 & v_M & 0 \\ 0 & 0 & v_M \end{pmatrix}, \quad (9)$$

$$\langle \Phi \rangle = \begin{pmatrix} v_2/\sqrt{2} & 0 \\ 0 & v_2/\sqrt{2} \end{pmatrix}. \quad (10)$$

These VEVs leave an unbroken $SU(2)_D$ custodial symmetry i.e. $SU(2)_L \times SU(2)_R \rightarrow SU(2)_D$. This ensures that $\rho = M_W^2/M_Z^2 \cos^2 \theta_W = 1$ at tree level and one now has

$$v = \sqrt{v_2^2 + 8v_M^2} \approx 246 \text{ GeV}. \quad (11)$$

As discussed in [5, 6], with respect to $SU(2)$, the two triplets (one real and one complex) and one doublet sum up to 13 degrees of freedom, 3 of which are Nambu-Goldstone bosons absorbed by W 's and Z leaving 10 physical degrees of freedom. Under the custodial symmetry $SU(2)_D$, these transform as

$$\text{five-plet (quintet)} \rightarrow H_5^{\pm\pm}, H_5^\pm, H_5^0;$$

$$\text{triplet} \rightarrow H_3^\pm, H_3^0;$$

$$\text{two singlets} \rightarrow H_1^0, H_1^{0'}$$

C. The seesaw mechanism in the $EW\nu_R$ model

The main purpose of the $EW\nu_R$ model was to provide a scenario in which right-handed neutrinos are non-sterile and get their masses out of the symmetry breaking of $SU(2) \times U(1)$. A Majorana mass term of the form $M_R \nu_R^T \sigma_2 \nu_R$ in the $EW\nu_R$ model comes from the following Yukawa interaction:

$$g_M l_R^{M,T} \sigma_2 \tilde{\chi} l_R^M, \quad (12)$$

which gives

$$g_M \nu_R^T \sigma_2 \nu_R \chi^0. \quad (13)$$

The right-handed neutrino Majorana mass is now intrinsically linked to the breaking scale of $SU(2) \times U(1)$ through the VEV of $\tilde{\chi}$ as

$$M_R = g_M v_M. \quad (14)$$

As stressed in [4], M_R is bounded from below because ν_R are now members of an $SU(2)$ doublet and would contribute to the Z-boson width leading to the lower bound:

$$M_R \geq M_Z/2 \approx 46 \text{ GeV} \quad (15)$$

A Dirac mass term is of the form $m_D(\nu_L^\dagger \nu_R + h.c.)$. This is a product of two doublets and the simplest choice for the Higgs scalar is an $SU(2)$ singlet with zero hypercharge, namely ϕ_S .

$$\mathcal{L}_S = g_{Sl} \bar{l}_L \phi_S l_R^M + H.c.. \quad (16)$$

With $\langle \phi_S \rangle = v_S$, the Dirac mass is given by

$$m_D = g_{Sl} v_S. \quad (17)$$

The magnitude of the light neutrino mass given by

$$m_\nu = \frac{m_D^2}{M_R} < O(eV), \quad (18)$$

implying $v_S \sim O(10^5 eV)$ if we assume $g_{Sl} \sim O(1)$ or $v_S \sim O(\Lambda_{EW} \sim 246 \text{ GeV})$ for $g_{Sl} \sim O(10^{-7})$.

D. Constraints from electroweak precision data

The presence of extra $SU(2)$ doublets of chiral fermions in the form of mirror fermions would seriously affect the constraints from electroweak precision data. As first mentioned in [4], the positive contribution of mirror fermions to the S-parameter could be compensated by the negative contribution to S from the Higgs triplets. A detailed analysis has been performed in [6] which showed that there is a large parameter space in the model which satisfies the present constraints of the electroweak precision data. A sample of the plots summarizing the scatter plots of the model is given below.

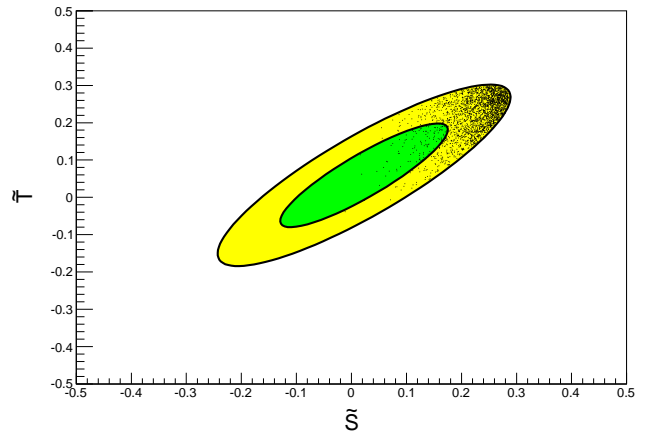


FIG. 1. Total \tilde{T} versus \tilde{S} with the 1 and 2 σ experimental contours

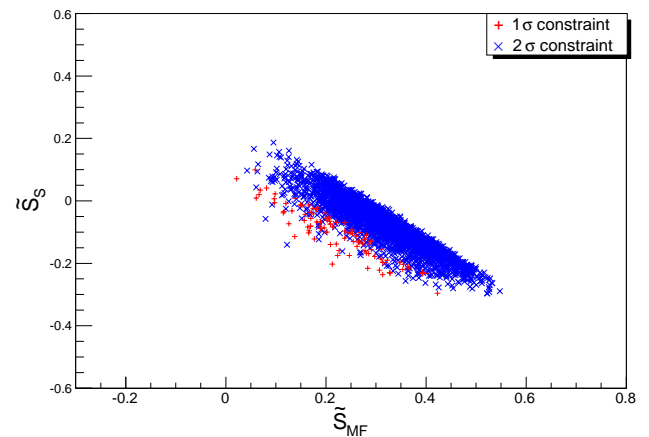


FIG. 2. Constrained \tilde{S}_S versus \tilde{S}_{MF}

In Fig. 1 \tilde{S} and \tilde{T} are new Physics contributions to the S and T parameters respectively. It is seen that the EW ν_R model satisfies very well the constraints from the electroweak precision data and has passed the first (indirect) test. In Fig. 2, \tilde{S}_S and \tilde{S}_{MF} refer to the contributions to S from the scalar and mirror fermion sectors respectively. Further details can be found in [6].

An important point which is worth repeating here is the role played by the scalar triplet in regulating the new physics contribution to the S-parameter. In fact, it has

been pointed out in [6] that the contribution to S from the scalar triplet can be made increasingly negative by increasing the mass of the doubly-charged Higgs as an example. This can offset the positive contribution coming from the mirror fermions. One can see the importance of the scalar sector, in particular the Higgs triplets, in making the $EW\nu_R$ model consistent with precision data.

The next step is to examine constraints coming from direct searches of the Higgs boson.

E. Constraint on the “minimal” $EW\nu_R$ model from the 126-GeV SM-like Higgs boson

By “minimal” we mean that the Higgs structure is as described above: one Higgs doublet and two Higgs triplets. Some phenomenology of these scalars has been investigated in [5]. This topic will be revisited in a future publication. For the purpose of this manuscript, we shall focus on the four neutral states: H_5^0 , H_3^0 , H_1^0 and $H_1^{0'}$ and in particular H_3^0 and H_1^0 since the other two do not couple to SM and mirror fermions [6]. H_3^0 and H_1^0 are CP-odd and CP-even respectively. As shown in [6], because of the coupling $g_{H_1^0 q\bar{q}} = -i\frac{m_q g}{2m_{WCH}}$, the gluon fusion production cross section for H_1^0 was estimated to be $\sigma_{EW\nu_R} \gtrsim 49\sigma_{SM}$ where the factor $49 = (1 + 6)^2$ takes into account the contributions from the top and mirror quarks. This alone practically ruled out H_1^0 as the 126-GeV SM-like scalar. Also, since the coupling to fermions are very similar to that of the SM, modulo the factor $1/\cos\theta_H$, the various branching ratios (BR) are expected to be of the order of those of the SM and the signal strengths ($\mu = (\sigma \times BR)/(\sigma \times BR)_{SM}$) will largely exceed observations.

It was shown in [6] that the CP-odd (pseudoscalar) H_3^0 could, with the appropriate choice of parameters, can fit the bill for being the 126-GeV object both in terms of the production cross section and in terms of branching ratios. However, a likelihood analysis ruled this option out by more than 3σ s [7]. Although a measurement of the spin and parity of the 126-GeV object is yet to be performed, it is fair to assume that it is more likely to be a 0^+ state.

As one can see, the reason why the CP-even H_1^0 has such a large gluon fusion production cross section (at least 49 times larger than the SM one at same mass) is because it comes from the Higgs doublet (the real part of the neutral component) which couples to SM fermions *as well as* mirror fermions. The loop controlling the gluon

fusion production of H_1^0 is dominated by the top quark and the mirror quarks giving rise to the factor of 49 mentioned above while it is dominated only by the top quark contribution in the SM. An extension in the Higgs sector of the minimal $EW\nu_R$ model is needed. This is shown in the next section.

III. EXTENDED $EW\nu_R$ MODEL

The simplest extension- and, in fact, the most natural one - of the minimal $EW\nu_R$ model is to have *two* Higgs doublets with one coupled to SM fermions and the other one to mirror fermions. To prevent cross coupling, a global symmetry will be imposed. Basically, we introduce the following Higgs doublets along with the corresponding global symmetries $U(1)_{SM} \times U(1)_{MF}$:

$$U(1)_{SM} : \Phi_2 \rightarrow e^{i\alpha_{SM}} \Phi_2 \\ (q_L^{SM}, l_L^{SM}) \rightarrow e^{i\alpha_{SM}} (q_L^{SM}, l_L^{SM}),$$

$$U(1)_{MF} : \Phi_{2M} \rightarrow e^{i\alpha_{MF}} \Phi_{2M} \\ (q_R^M, l_R^M) \rightarrow e^{i\alpha_{MF}} (q_R^M, l_R^M),$$

$$\phi_S \rightarrow e^{-i(\alpha_{MF} - \alpha_{SM})} \phi_S, \quad (19)$$

$$\tilde{\chi}, \xi \rightarrow e^{-2i\alpha_{MF}} \tilde{\chi}, \xi. \quad (20)$$

All other fields ($SU(2)$ -singlet right-handed SM fermions, left-handed mirror fermions) are singlets under $U(1)_{SM} \times U(1)_{MF}$.

These symmetries will forbid, at tree level, Yukawa couplings of the form $g_Y \bar{f}_L \Phi_2 M f_R$ and $g_Y \bar{f}_R^M \Phi_2 f_L^M$. Only Yukawa interactions of the type $g_Y \bar{f}_L \Phi_2 f_R$ and $g_Y \bar{f}_R^M \Phi_{2M} f_L^M$ are allowed. The Yukawa couplings of the physical states to SM and mirror fermions will involve mixing angles. This is detailed in the Appendix A.

About the extended scalar sector. One now has one extra Higgs doublet which leads to 4 more degrees of freedom. The physical states of custodial $SU(2)_D$ are:

$$\text{five-plet (quintet)} \rightarrow H_5^{\pm\pm}, H_5^\pm, H_5^0;$$

$$\text{two triplets} \rightarrow H_3^\pm, H_3^0; H_{3M}^\pm, H_{3M}^0;$$

$$\text{three singlets} \rightarrow H_1^0, H_{1M}^0, H_1^{0'}$$

The three singlet states H_1^0 , H_{1M}^0 and $H_1^{0'}$ can have mass mixings. (A detailed discussion of the potential and various physical states is given in the Appendix A.) The

scalar mass eigenstates will be a mixture of these three states, and it is where we will focus on in the next two sections.

IV. COMPARING EW ν_R MODEL PREDICTIONS WITH DATA

Measured properties of the 126 GeV scalar particle that was discovered at the LHC so far tend to be close to the properties of SM Higgs boson. Hence, in every model of BSM Physics it is imperative to (i) have at least one Higgs particle with about 126 GeV having SM-like decay properties, and (ii) study the implications of these properties in the ‘allowed’ parameter space of the model (e.g. allowed masses of any BSM particles in the model, etc.). To check the viability of a model or to search for the model experimentally, decay properties of the 126 GeV Higgs boson candidate in the model must be studied.

The cross section of any decay channel of the Higgs boson that is measured at the LHC is given by

$$\sigma(H\text{-decay}) = \sigma(H\text{-production}) \times BR(H\text{-decay}), \quad (21)$$

where $\sigma(H\text{-production})$ is the production cross section of H and $BR(H\text{-decay})$ is the Branching Ratio of the decay channel of H that is under consideration.

$$BR(H\text{-decay}) = \frac{\Gamma(H\text{-decay})}{\Gamma_H}, \quad (22)$$

where $\Gamma(H\text{-decay})$ is the partial width of the H -decay channel, and Γ_H is the total width of H . Because the decay widths $\Gamma(H\text{-decay})$ cannot be experimentally measured, we compare $\sigma_{H\text{-decay}}$ in the EW ν_R model with the predictions SM for that decay channel. So we define the well known signal strength

$$\mu(H\text{-decay}) = \frac{\sigma(H\text{-decay})}{\sigma_{SM}(H\text{-decay})}, \quad (23)$$

$\sigma(H\text{-decay})$ being measured experimentally or predicted by a model.

As seen in Appendix A, the EW ν_R model has 6 neutral physical scalars, of which 3 are CP-even states (H_1^0, H_{1M}^0, H_1') and 3 are CP-odd states (H_3^0, H_{3M}^0, H_5^0). Their couplings to fermions and gauge bosons are listed in Tables VI - X in Appendix A. Among these H_5^0 does not couple to charged fermions. It can be seen from Table VI that decay widths of $H_3^0/H_{3M}^0 \rightarrow f \bar{f}$ can be close to the SM predictions for some combinations of the BSM parameters in the couplings. But as mentioned in Section II E, H_3^0, H_{3M}^0 are disfavored as 126 GeV candidates

as compared to the CP-even hypothesis [7]. Hence, in this paper while considering 126 GeV candidate in the EW ν_R model, we proceed with the hypothesis that this candidate is a CP-even eigenstate¹. Out of the 3 CP-even Higgs bosons, only H_1^0 can have decay widths to SM fermions similar to the SM predictions. Therefore, one might expect that in the EW ν_R model H_1^0 is the candidate to be 126 GeV Higgs boson. But it is not that simple!

Because the three custodial singlet scalars can mix, according to Eq. (A24), generally, H_1^0 is not a mass eigenstate. To obtain the mass eigenstates including the actual 126 GeV candidate in this model, we need to diagonalize the mass matrix in Eq. (A24). Thus, after the electroweak symmetry breaking the $SU(2)_D$ singlet mass eigenstates are given by:

$$\begin{pmatrix} \tilde{H} \\ \tilde{H}' \\ \tilde{H}'' \end{pmatrix} = \begin{pmatrix} a_{1,1} & a_{1,1M} & a_{1,1'} \\ a_{1M,1} & a_{1M,1M} & a_{1M,1'} \\ a_{1',1} & a_{1',1M} & a_{1',1'} \end{pmatrix} \begin{pmatrix} H_1^0 \\ H_{1M}^0 \\ H_1^{0'} \end{pmatrix}. \quad (24)$$

We denote these mass eigenstates by \tilde{H}, \tilde{H}' , and \tilde{H}'' . Their masses depend on elements of the mixing matrix, and their decay properties also depend on other parameters as shown in Appendix A. The vacuum expectation values (VEVs) of the real parts of Φ_2, Φ_{2M} and χ are also among these parameters, and need to be varied to find different cases of 126 GeV candidates in this model. Hence, it is necessary to estimate the limits on these VEVs before analyzing 126 GeV candidates in detail.

Limits on VEVs:

Recall that the VEVs of the real parts of Φ_2, Φ_{2M} and χ are $(v_2/\sqrt{2}), (v_{2M}/\sqrt{2})$ and v_M respectively. The charged SM fermions, the charged mirror fermions and the right handed neutrinos get their masses due to v_2, v_{2M} , and v_M respectively. Various constraints on these masses constrain the ranges of the VEVs.

If the pole mass of top quark (173.5 GeV), the heaviest SM fermion, is *perturbative* and comes from v_2 , then $v_2 \gtrsim 69$ GeV (because $g_{top}^2 \leq 4\pi$). We set the lower bound on the masses of all the charged mirror fermions

¹ The possibility that the 126 GeV Higgs boson is a linear combination of CP-even and CP-odd state has not been thoroughly checked experimentally yet. The spin and parity of the 126 GeV scalar are yet to be measured at CMS and ATLAS. Thus, in this paper, we will stick to CP-eigenstate hypothesis based on the likelihood analysis

at 102 GeV, which is the LEP3 [16] bound on the heavy BSM quarks and BSM charged leptons. Hence, considering a constraint of $g_{MF}^2/4\pi \leq 1.5$ on the Yukawa couplings of all the charged mirror fermions, $v_{2M} \gtrsim 27$ GeV, implying $v_M \lesssim 80$ GeV. Thus, for M_R to be perturbative $M_R \lesssim 283$ GeV. We also know that $M_R \geq M_Z/2 \approx 45.5$ GeV [4], and, hence, $v_M \gtrsim 13$ GeV. This implies that $v_2, v_{2M} \lesssim 234$ GeV. The allowed ranges for VEVs and for parameters defined in Eq (A8) are summarized in the table below. Keeping all this in mind we are now

TABLE I. Allowed ranges of VEVs and parameters defined in Eq. (A8). All values are given in GeV .

$69 \lesssim v_2 \lesssim 234$	$0.28 \lesssim s_2 \lesssim 0.95$
$27 \lesssim v_{2M} \lesssim 234$	$0.11 \lesssim s_{2M} \lesssim 0.95$
$13 \lesssim v_M \lesssim 80$	$0.15 \lesssim s_M \lesssim 0.91$

ready to analyze in detail the decay properties of the 126 GeV candidate in the EW ν_R model.

V. 126 GEV CANDIDATE IN EW ν_R MODEL

In the EW ν_R model the lightest of \tilde{H} , \tilde{H}' or \tilde{H}'' can be a candidate for 126 GeV Higgs boson. Hereafter, we will denote it by \tilde{H} ; the next heavier mass eigenstate will be denoted by \tilde{H}' , and the heaviest one by \tilde{H}'' . From Eq. (24) we see that each of these three mass eigenstates is a mixture of custodial singlet scalars H_1^0 , H_{1M}^0 and $H_1^{0'}$. Recall that H_1^0 comes from the SM-like scalar doublet Φ_2 , H_{1M}^0 comes from doublet Φ_{2M} and $H_1^{0'}$ from triplet χ . Because measured decay properties of the 126 GeV Higgs boson are close to SM predictions, intuitively one might expect that H_1^0 has to be the dominant component of \tilde{H} . But our investigation shows that the 126 GeV \tilde{H} can have SM-like decay properties, even if H_1^0 is a sub-dominant component in it. Hence, the dual-like nature of 126 GeV Higgs boson from perspective of the EW ν_R model. In this section we will discuss this dual-like nature and its implications for the scalar sector in this model.

A. \tilde{H} as 126 GeV Higgs candidate with a dominant H_1^0 component

We can vary the elements of the mass matrix in Eq. (A24) to find those numerical forms of the mixing matrix

in Eq. (24), such that, after the electroweak symmetry breaking, one of the three singlet mass eigenstates has a mass around 126 GeV and two other states are heavier. The λ 's in the mass matrix can be chosen such that the 126 GeV state has a dominant H_1^0 component. In this subsection we will discuss two example scenarios in which \tilde{H} acquires a mass of about 126 GeV. For both the scenarios $s_2 = 0.92$, $s_{2M} = 0.16$, $s_M \approx 0.36$:

Example 1: $\lambda_1 = -0.077$, $\lambda_2 = 14.06$, $\lambda_3 = 15.4$, $\lambda_4 = 0.1175$,

$$\begin{pmatrix} \tilde{H} \\ \tilde{H}' \\ \tilde{H}'' \end{pmatrix} = \begin{pmatrix} 0.998 & -0.0518 & -0.0329 \\ 0.0514 & 0.999 & -0.0140 \\ 0.0336 & 0.0123 & 0.999 \end{pmatrix} \begin{pmatrix} H_1^0 \\ H_{1M}^0 \\ H_1^{0'} \end{pmatrix}, \quad (25)$$

with $m_{\tilde{H}} = 125.7$ GeV, $m_{\tilde{H}'} = 420$ GeV, $m_{\tilde{H}''} = 601$ GeV.

Example 2: $\lambda_1 = 0.0329$, $\lambda_2 = 14.2$, $\lambda_3 = 15.4$, $\lambda_4 = 0.0056$,

$$\begin{pmatrix} \tilde{H} \\ \tilde{H}' \\ \tilde{H}'' \end{pmatrix} = \begin{pmatrix} 0.99999\dots & -2.49 \times 10^{-3} & -1.60 \times 10^{-3} \\ 2.49 \times 10^{-3} & 0.99999\dots & -5.30 \times 10^{-4} \\ 1.60 \times 10^{-4} & 5.26 \times 10^{-4} & 0.99999\dots \end{pmatrix} \begin{pmatrix} H_1^0 \\ H_{1M}^0 \\ H_1^{0'} \end{pmatrix}. \quad (26)$$

with $m_{\tilde{H}} = 125.7$ GeV, $m_{\tilde{H}'} = 420$ GeV, $m_{\tilde{H}''} = 599$ GeV.

Fixing the aforementioned parameters fully determines the numerical form of the custodial singlet scalar mixing matrix. In these two scenarios, H_1^0 is the most dominant component in \tilde{H} and $H_{1M}^0, H_1^{0'}$ are highly sub-dominant components. Thus, $\tilde{H} \approx H_1^0$ i.e. it almost entirely originates from SM-like $SU(2)$ scalar doublet Φ_2 . But, still, the scalar spectrum is not entirely SM-like, since heavier \tilde{H}' and \tilde{H}'' also exist. These are not the only two scenarios which can give $m_{\tilde{H}} \approx 126$ GeV, but are merely two examples.

For a spectrum like this, where $m_{\tilde{H}} \approx 126$ GeV $<$ $m_{\tilde{H}'}$ $<$ $m_{\tilde{H}''}$, we calculate the partial widths of various decay channels as explained in Appendix B. We calculate the total width of \tilde{H} by adding individual partial widths:

$$\begin{aligned} \Gamma_{\tilde{H}} = & \Gamma_{\tilde{H} \rightarrow b\bar{b}} + \Gamma_{\tilde{H} \rightarrow \tau\bar{\tau}} + \Gamma_{\tilde{H} \rightarrow c\bar{c}} + \Gamma_{\tilde{H} \rightarrow W^+W^-} \\ & + \Gamma_{\tilde{H} \rightarrow ZZ} + \Gamma_{\tilde{H} \rightarrow gg} + \Gamma_{\tilde{H} \rightarrow \gamma\gamma}. \end{aligned} \quad (27)$$

Among all the partial widths considered above, $\Gamma_{\tilde{H} \rightarrow b\bar{b}}$ and $\Gamma_{\tilde{H} \rightarrow W^+W^-}$ are the most dominant. Note that at

126 GeV mass $\tilde{H} \rightarrow f^M \bar{f}^M$ decays do not come into the picture, because $m_{f^M} > 100$ GeV implies that these are not kinematically possible decays at the tree level. We will discuss more about this constraint shortly.

After fixing the singlet-scalar mixing matrix (as in Eqs. (25, 26)), a few other parameters for the signal strength calculation can still be varied independently. Calculation of the partial width of $\tilde{H} \rightarrow \gamma\gamma$ channel necessitates fixing the values or ranges for the remaining parameters. In both Examples 1 and 2 (Eq (25,26) respectively), we fix other parameters as follows:

- $m_{H_3^+} = 600$ GeV, $m_{H_{3M}^+} = 700$ GeV,
- masses of all three charged mirror leptons $m_{lM} = 102$ GeV,
- mass of lightest two generations of mirror quarks $m_{q_1^M} = m_{q_2^M} = 102$ GeV,
- for the purpose of partial widths of \tilde{H} -decays in scenarios above, we also fix mass of the third mirror quark generation at $m_{qM} = 120$ GeV. This mass will be varied to analyze constraints on $\tilde{H} \sim H_{1M}^0$.

The values of $m_{H_3^+}$ and $m_{H_{3M}^+}$ are chosen so as to have largest allowed ranges for $m_{H_5^0}$ and $m_{5^{++}}$. We vary the latter two over the range $\sim 400 - 730$ GeV for Example 1 and 2.

The lower limit of 102 GeV on masses of charged mirror leptons and mirror quarks is imposed based on the results of search for sequential heavy charged leptons and quarks at LEP3 (refer 'Heavy Charged Leptons' and 'Heavy Quarks' sections in [16] and references therein). Strictly speaking these constraints apply only to sequential-like heavy BSM fermions, because searches for charged heavy leptons and heavy quarks are done specifically for sequential-like heavy fermions, e.g. heavy charged leptons L' decaying as $L' \rightarrow \tau Z$. However, charged mirror fermions in the $EW\nu_R$ model couple to the SM fermions in an altogether different way, through the scalar singlet ϕ_S [4, 19]. Still, we impose these constraints on charged mirror fermions in this model, arguing that if these mirror fermions were lighter than ~ 100 GeV, they would have been discovered at LEP3.

Fig. 3 shows the comparison of CMS data for signal strengths $\mu(H\text{-decay})$ of the 126 GeV Higgs boson, and the predictions of those signal strengths for the 126 GeV \tilde{H} in Examples 1 and 2, put together. For predictions in the $EW\nu_R$ model we have considered the gluon-gluon fusion production channel ($gg \rightarrow \tilde{H}$), which is the most

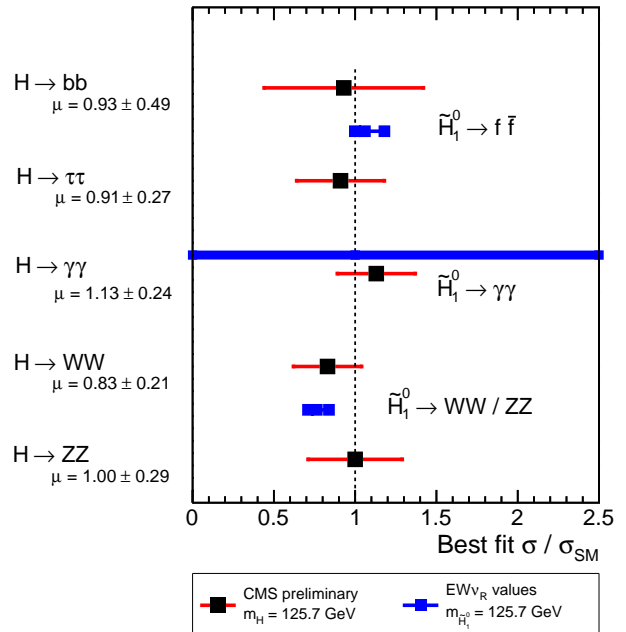


FIG. 3. The figure shows predictions of $\mu(\tilde{H} \rightarrow W^+W^-, ZZ, b\bar{b}, \tau\bar{\tau})$ by $EW\nu_R$ model in $\tilde{H} \sim H_1^0$ scenario for varying three slightly different forms of the singlet mixing matrix, in comparison with corresponding best fit values by CMS.

dominant Higgs-production channel at the LHC. Table II shows a summary of properties of 126 GeV Higgs at CMS and predictions for those properties in the $EW\nu_R$ model. Calculation of the predicted values is explained in Appendix B. A few comments are in order here in context of Fig. 3. It can be seen that the $EW\nu_R$ model predictions for $\mu(\tilde{H} \rightarrow W^+W^-, ZZ)$ are the equal, and similarly predictions for $\mu(\tilde{H} \rightarrow b\bar{b}, \tau\bar{\tau})$ are the equal. This is expected, since as seen in Appendix B,

$$\frac{\Gamma^{EW\nu_R}(\tilde{H} \rightarrow W^+W^-)}{\Gamma^{SM}(H_{SM}^0 \rightarrow W^+W^-)} = \frac{\Gamma^{EW\nu_R}(\tilde{H} \rightarrow ZZ)}{\Gamma^{SM}(H_{SM}^0 \rightarrow ZZ)},$$

$$\frac{\Gamma^{EW\nu_R}(\tilde{H} \rightarrow b\bar{b})}{\Gamma^{SM}(H_{SM}^0 \rightarrow b\bar{b})} = \frac{\Gamma^{EW\nu_R}(\tilde{H} \rightarrow \tau\bar{\tau})}{\Gamma^{SM}(H_{SM}^0 \rightarrow \tau\bar{\tau})}. \quad (28)$$

Different predictions for μ of each channel in Fig. 3 (different blue squares along a horizontal blue line) are for different values of $a_{1,1M}$.

Notice that we draw a blue line over the entire horizontal range for $\mu(\tilde{H} \rightarrow \gamma\gamma)$. This is, because over the ranges of $m_{H_5^+}$ and $m_{H_5^{++}}$, $\mu(\tilde{H} \rightarrow \gamma\gamma)$ can easily vary in the range $[0, 2.5]$ without significantly affecting ranges of the signal strengths for other decay channels. The vari-

TABLE II. $\mu = \sigma/\sigma_{SM}$ for decay channels as measured at CMS and as calculated in $EW\nu_R$ model in $gg \rightarrow \tilde{H}$ channel for given values of the parameters.

Decay Channel	Observed μ at CMS	Calculated μ ($\sim 5\%$ accuracy) for 126 GeV \tilde{H} $a_{1,1M} = -0.0555$ to -0.0533 (-0.0025 to -0.00014)
WW	0.83 ± 0.21 (ggH, VBF, VH channels) [11]	$0.83 - 0.71$ ($0.71 - 0.84$)
ZZ	1.00 ± 0.29 (ggH, VBF, $t\bar{t}H$, VH channels) [12]	$0.83 - 0.71$ ($0.71 - 0.84$)
$\tau\tau$	0.91 ± 0.27 (non-VH channels) [14]	$1.18 - 1.01$ ($1.00 - 1.18$)
bb	0.93 ± 0.49 (VH channels) [13]	$1.18 - 1.01$ ($1.00 - 1.18$)

ation of $\mu(\tilde{H} \rightarrow \gamma\gamma)$ with $m_{H_5^+}$ and $m_{H_5^{++}}$ can be seen in Figs. 4, 5. For completion we show a contour plot of $\mu(\tilde{H} \rightarrow \gamma\gamma) = 1$ in $m_{H_5^\pm}, m_{H_5^{\pm\pm}}$ plane for Examples 1 and 2 in Figs. 6, 7 respectively. Thus, we can conclude that in $\tilde{H} \approx H_1^0$ scenario predictions of the $EW\nu_R$ model agree with the properties of 126 GeV Higgs boson, as measured by CMS and ATLAS. However, individual partial decay widths and branching ratios of \tilde{H} can be very different from the SM Higgs boson. Therefore, more data and further analysis of partial decay widths of the 126 GeV Higgs boson at the LHC are required to make a conclusive statement about whether it is a SM Higgs or just a SM-lookalike ‘‘impostor’’ \tilde{H} in the $EW\nu_R$ model.

In addition to studying decay properties of the 126 GeV Higgs boson, the search for SM-like heavy Higgs bosons has also been carried out at CMS and ATLAS in decay channels like W^+W^- [30] and $\gamma\gamma$ [22]. In the two example scenarios considered above the next heavier state after 126 GeV turns out to be \tilde{H}' , and \tilde{H}'' is the heaviest. \tilde{H}' couples to all the particles that SM Higgs boson couples to and it is also a CP-even state. Thus, constraints on a SM-like heavy Higgs boson may also constrain \tilde{H}' . While varying the mass of \tilde{H}' over the range [150, 650] GeV, we compared the signal strength of $\tilde{H}' \rightarrow W^+W^-$ [18, 30] and $\sigma(gg \rightarrow \tilde{H}') \times BR(\tilde{H}' \rightarrow \gamma\gamma)$ [21, 22] in the $EW\nu_R$ model to the constraints from heavy Higgs search in W^+W^- and $\gamma\gamma$ decay channels at CMS.

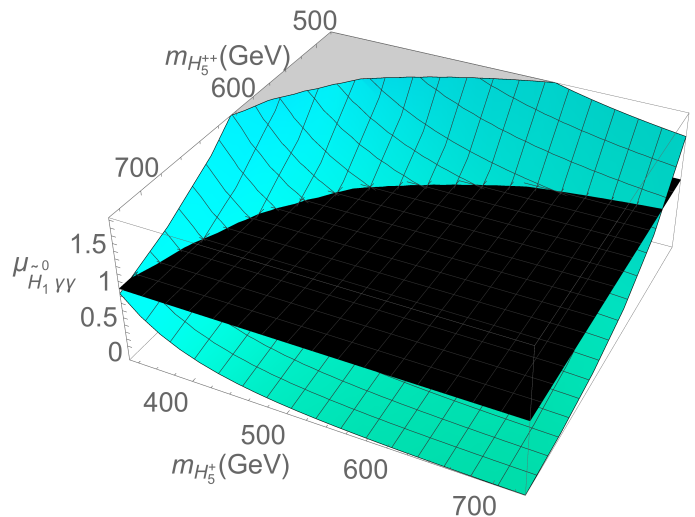


FIG. 4. $\mu(\tilde{H} \rightarrow \gamma\gamma)$ for $m_{H_3^\pm} = 600$ GeV, $a_{1,1M} = -0.0518$.

We calculated the total width of \tilde{H}' using

$$\begin{aligned}
 \Gamma_{\tilde{H}'} &= \sum_{i=1}^3 \Gamma_{\tilde{H}' \rightarrow q_i^M \bar{q}_i^M} + \sum_{j=1}^3 \times \Gamma_{\tilde{H}' \rightarrow l_j^M \bar{l}_j^M} \\
 &+ \Gamma_{\tilde{H}' \rightarrow t\bar{t}} + \Gamma_{\tilde{H}' \rightarrow b\bar{b}} \\
 &+ \Gamma_{\tilde{H}' \rightarrow \tau\bar{\tau}} + \Gamma_{\tilde{H}' \rightarrow c\bar{c}} + \Gamma_{\tilde{H}' \rightarrow W^+W^-} \\
 &+ \Gamma_{\tilde{H}' \rightarrow ZZ} + \Gamma_{\tilde{H}' \rightarrow gg} + \Gamma_{\tilde{H}' \rightarrow \gamma\gamma}. \quad (29)
 \end{aligned}$$

Partial decay widths were calculated using the method illustrated in Appendix B. The constraints on $\sigma(gg \rightarrow$

TABLE III. Comparison of production cross-section and branching ratios for various channels in SM and the $EW\nu_R$ model for Example 2 scenario: $a_{1,1M} = -0.0025$, where 126 GeV $\tilde{H} \sim H_1^0$.

	SM			$EW\nu_R$			$\mu = \frac{(\sigma_{Hgg} \times BR)_{SM}}{(\sigma_{\tilde{H}gg} \times BR)_{EW\nu_R}}$
	$\Gamma_{H \rightarrow gg}$ $\propto \sigma_{gg \rightarrow H}$	BR	$\Gamma_{Hgg} \times BR$	$\Gamma_{\tilde{H} \rightarrow gg}$ $\propto \sigma_{gg \rightarrow H}$	BR	$\Gamma_{\tilde{H}gg} \times BR$	
$\tilde{H} \rightarrow WW$	3.55E-04	2.26E-01	8.02E-05	3.46E-04	1.77E-01	6.12E-05	0.76
$\tilde{H} \rightarrow ZZ$	3.55E-04	2.81E-02	9.97E-06	3.46E-04	2.20E-02	7.61E-06	0.76
$\tilde{H} \rightarrow bb$	3.55E-04	5.66E-01	2.01E-04	3.46E-04	6.21E-01	2.15E-04	1.07
$\tilde{H} \rightarrow \tau\tau$	3.55E-04	6.21E-02	2.20E-05	3.46E-04	6.82E-02	2.36E-05	1.07
$\tilde{H} \rightarrow \gamma\gamma$	3.55E-04	2.28E-03	8.09E-07	3.46E-04	2.99E-03	1.03E-06	1.28

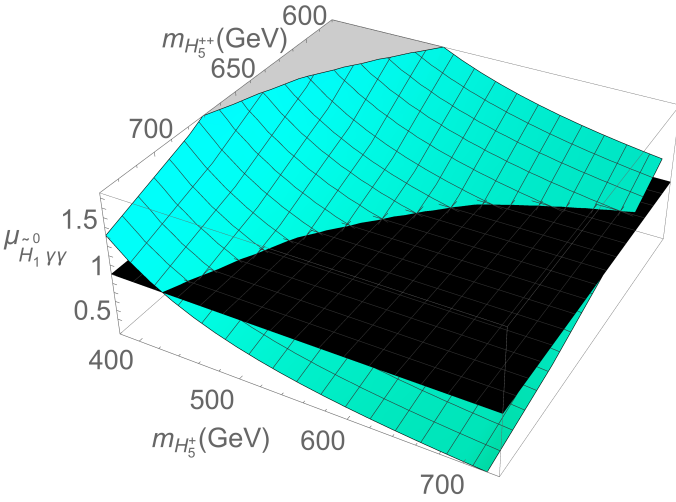


FIG. 5. $\mu(\tilde{H} \rightarrow \gamma\gamma)$ for $m_{H_3^\pm} = 600$ GeV, $a_{1,1M} = -0.0025$.

H^0) $\times BR(H^0 \rightarrow \gamma\gamma)$ in [22] are accompanied by assumptions that total width of the SM-like heavy Higgs $\Gamma_{H^0} = 0.1$ GeV or 10% of mass of H^0 . Although the total width of \tilde{H}' in our scenarios does not follow either of these patterns, we observed that $\sigma(gg \rightarrow \tilde{H}') \times BR(\tilde{H}' \rightarrow \gamma\gamma)$ predictions in example 1 and 2 were consistently lower than the CMS constraints.

On the other hand imposing the constraints from SM-like heavy Higgs search on the signal strength of $\tilde{H}' \rightarrow W^+W^-$, throughout the mass range [150, 650] GeV is not as trivial as it might appear at the first sight. Fig 8 shows $\mu(\tilde{H}' \rightarrow W^+W^-)$ for $\Gamma_{\tilde{H}'} \lesssim m_{\tilde{H}'}$, with CMS results of SM-like heavy Higgs boson search in W^+W^- decay channel. $\alpha_{fM} = g_{Yukawa}^2/4\pi$ is the Yukawa coupling constant for the charged mirror fermions. This plot should be interpreted as follows. The data at CMS is already sen-

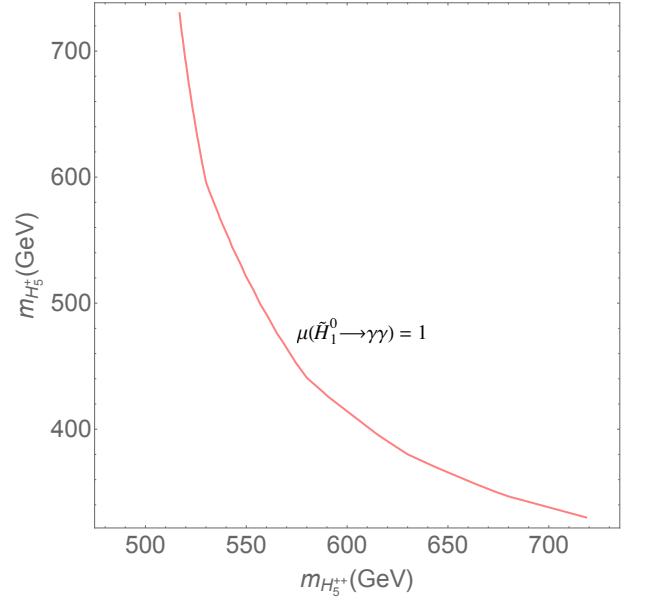


FIG. 6. $\mu(\tilde{H} \rightarrow \gamma\gamma)$ contour plot, where $\sigma(\tilde{H} \rightarrow \gamma\gamma) = \sigma(H_{SM} \rightarrow \gamma\gamma)$ for $m_{H_3^\pm} = 600$ GeV, $a_{1,1M} = -0.0518$.

sitive to the region of $\mu(H_{SM-like} \rightarrow W^+W^-)$ -vs.- m_{H^0} parameter space that is above the 2σ background bands, with 95% Confidence Level (CL). Thus, absence of any observed resonance above the background in the data rules out a SM-like Higgs in this part of the parameter space. However, the data is not yet conclusive about the parameter space around or below the 2σ background bands. But with more data, when the background bands required to make a 95% CL distinction between signal and background are expected to gradually shift downward, a conclusive statement can be made about this region of $\mu(H^0 \rightarrow W^+W^-)$ -vs.- m_{H^0} parameter space.

The search at CMS looks for a heavy SM-like Higgs

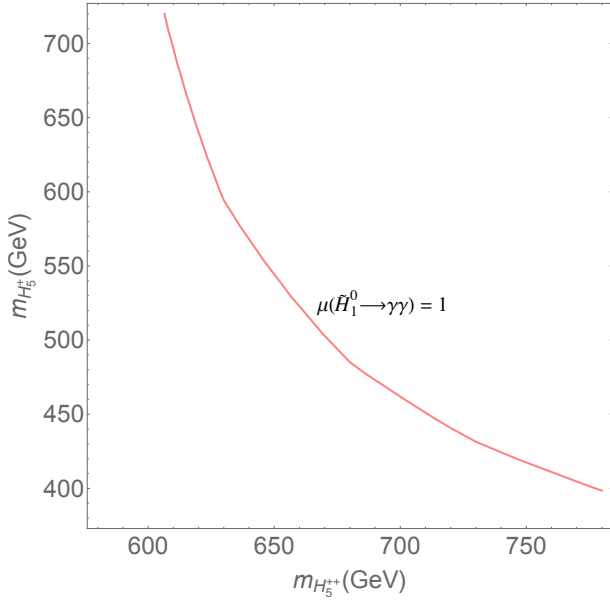


FIG. 7. $\mu(\tilde{H} \rightarrow \gamma\gamma)$ contour plot, where $\sigma(\tilde{H} \rightarrow \gamma\gamma) = \sigma(H_{SM} \rightarrow \gamma\gamma)$ for $m_{H_3^\pm} = 600$ GeV, $a_{1,1M} = -0.0025$.

that might appear as a resonance in excess to the background. Such a resonance can be seen if the total width of the particle is much smaller than its mass. In Examples 1 and 2 the total width of \tilde{H}' exceeds its mass after it crosses the ($2 \times$ mirror fermion mass) threshold. When the total width of a particle becomes comparable to its width, the particle can no longer appear as a resonance over the background. A well known example of such a phenomenon is the sigma model of QCD, where the sigma particle cannot be seen experimentally as a resonance. In Fig. 8, on the left side of this curve the signal strength of $\tilde{H}' \rightarrow W^+W^-$ is consistently greater than 2σ background bands and the data. Hence, in this mass range \tilde{H}' is excluded for scenarios similar to Examples 1 and 2. But we cannot make such a conclusive statement about the region beyond the red dots on the blue curves. In this region, $\Gamma_{\tilde{H}'} > m_{\tilde{H}'}$ and $m_{\tilde{H}'} > 2 \times$ mirror fermion masses. Therefore, if the total width of \tilde{H}' is calculated using Eq. (29), it turns out to be highly dominated by $\Gamma_{\tilde{H}' \rightarrow f^M \bar{f}^M}$. Hence, in this mass range \tilde{H}' is not expected to show up as a resonance above the background. To make a concrete prediction of \tilde{H}' signal strengths in this mass range, it should be treated like a strongly coupled Higgs, and the partial width calculations would involve form factors of $\tilde{H}' f^M \bar{f}^M$ interactions. This analysis is out of the scope of this paper and could be of interest for future work. But this implies that the constraints from SM-like heavy Higgs search at CMS cannot be imposed

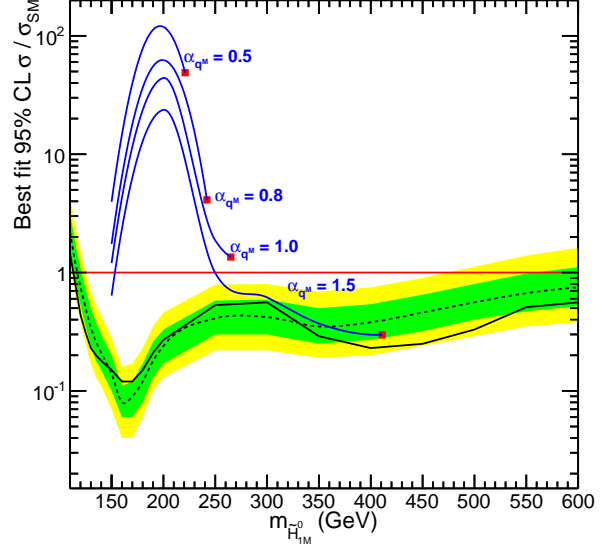


FIG. 8. $a_{1,1M} = -0.0518$; The graph shows variation of $\mu(\tilde{H}' \rightarrow W^+W^-)$ with the mass of \tilde{H}' in the range 150 - 600 GeV for different values of $g_{H_{1M} f^M f^M}^2/4\pi$ (0.5, 0.8, 1.0, 1.5 from top blue curve downward respectively), where $g_{H_{1M} f^M f^M}$ is the Yukawa coupling of H_{1M} with the mirror fermions. This overlaps the results of search for SM-like Higgs boson up to 600 GeV with the 1σ (green band) and 2σ (yellow band) limits on the 'SM' background (dotted curve) and the data at CMS (solid black curve). Vertical dotted line is drawn to indicate that CMS data is available only up to 600 GeV .

on \tilde{H}' when $\Gamma_{\tilde{H}'} > m_{\tilde{H}'}$.

For completion a few remarks about \tilde{H}'' should be made here. Although \tilde{H}'' also couples to all the particles that SM-Higgs boson couples to, in Example scenarios 1 and 2 considered here $m_{\tilde{H}''} \sim 600$ GeV. And it can be seen from the CMS data in Fig 8 that the data available in this mass range and beyond is not enough to be sensitive to signal strength of the order of SM predictions. Also, $\tilde{H}'' \sim H_1^0$, which means that it couples to SM charged fermions very weakly. Hence, more data is required to study \tilde{H}'' in this heavy mass range.

To summarize this subsection, we have so far explored the possibility that H_1^0 is the dominant component in 126 GeV \tilde{H} in the EW ν_R model. We showed that the 126 GeV Higgs boson at the LHC could be $\tilde{H} \sim H_1^0$, and more data and analysis are required to confirm or rule out this possibility. Within the regime of EW ν_R model \tilde{H}' can be the next heavier neutral scalar particle after 126 GeV . Based on the results of the search for

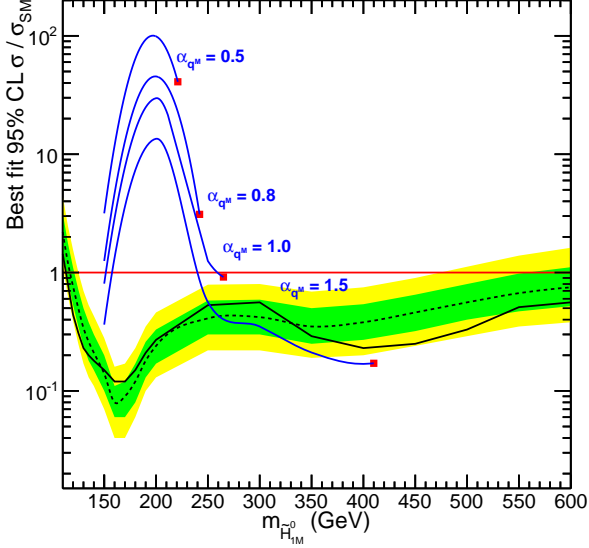


FIG. 9. $a_{1,1M} = -0.0025$; The graph shows variation of $\mu(\tilde{H}' \rightarrow W^+W^-)$ with the mass of \tilde{H}' in the range 150 - 600 GeV for different values of $g_{H_{1M}^2 f^M f^{M'}}/4\pi$ (0.5, 0.8, 1.0, 1.5 from top blue curve downward respectively), where $g_{H_{1M}^2 f^M f^{M'}}$ is the Yukawa coupling of H_{1M} with the mirror fermions. This overlaps the results of search for SM-like Higgs boson up to 600 GeV with the 1σ (green band) and 2σ (yellow band) limits on the 'SM' background (dotted curve) and the data at CMS (solid black curve). Vertical dotted line is drawn to indicate that CMS data is available only up to 600 GeV .

SM-like heavy Higgs boson at CMS a lower limit of $\sim 250 - 400$ GeV can be set on \tilde{H}' . In the mass range heavier than this limit, the total width of \tilde{H}' exceeds its mass and hence, it should be treated like a strongly coupled scalar (strong coupling to the mirror fermions). The current data cannot really put a stringent constraint on \tilde{H}' in this heavier mass range.

B. \tilde{H} as 126 GeV Higgs candidate with H_1^0 as a sub-dominant component

The question we explore in this subsection is: 'can 126 GeV \tilde{H} in the $EW\nu_R$ model have H_1^0 as a subdominant component?' There are only two CP-even, neutral scalar states other than H_1^0 , and they are H_{1M}^0 and $H_1^{0'}$. This sounds counter-intuitive, since H_1^0 is the only scalar state that entirely arises from SM-like $SU(2)$ scalar doublet. But to be thorough, we scanned the relevant parameter space to find out if H_{1M}^0 or $H_1^{0'}$ can, indeed, be

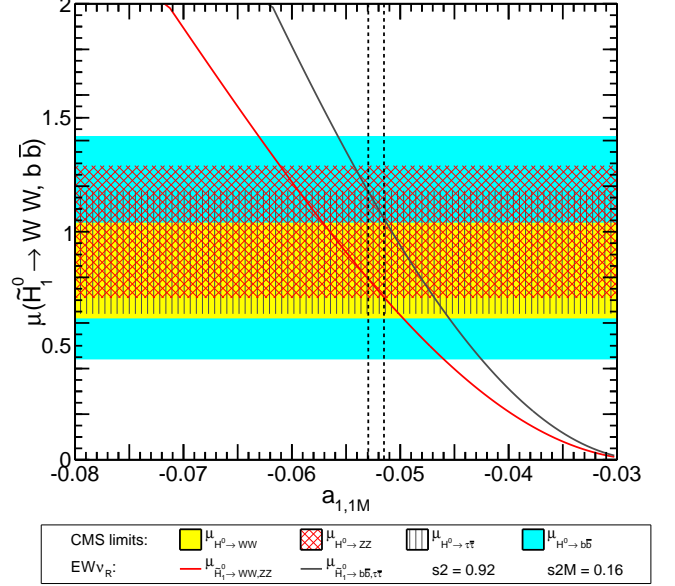


FIG. 10. The graph shows how $\mu(\tilde{H} \rightarrow WW, ZZ)$ and $\mu(\tilde{H} \rightarrow ff)$ vary with ' $a_{1,1M}$ '. The shaded areas show limits on μ 's for different channels from data at CMS (refer to Table II). The two leftmost black dashed lines (and two rightmost lines) enclose a range of $a_{1,1M}$ that is consistent with all the constraints analyzed in this paper including those coming from $\tilde{H}' \rightarrow WW$.

the dominant components in 126 GeV \tilde{H} while agreeing with the measured signal strengths of the 126 GeV Higgs at the LHC. We address this problem in two steps:

- Is it possible for \tilde{H} to obtain a mass of about 126 GeV with H_1^0 as a subdominant?
- If yes, can such a 126 GeV physical scalar agree with the measured signal strengths of 126 GeV Higgs boson at LHC?

To address the first question, we adopted the following method. The relevant parameters which enter this calculation are given below Eq (A24), along with their ranges.

$$\begin{aligned}
 -4\pi &\leq \lambda_1, \lambda_2, \lambda_3, \lambda_4 \leq 4\pi, \\
 0.28 &\leq s_2 \leq 0.95, \\
 0.11 &\leq s_{2M} \leq 0.95, \\
 0.15 &\leq s_M \leq 0.91.
 \end{aligned} \tag{30}$$

Here, the limits for λ 's are set so that $\lambda/4\pi \sim 1$, for perturbativity. Limits on s_2, s_{2M}, s_M are based on table I. We randomly generated value of each of these parameters

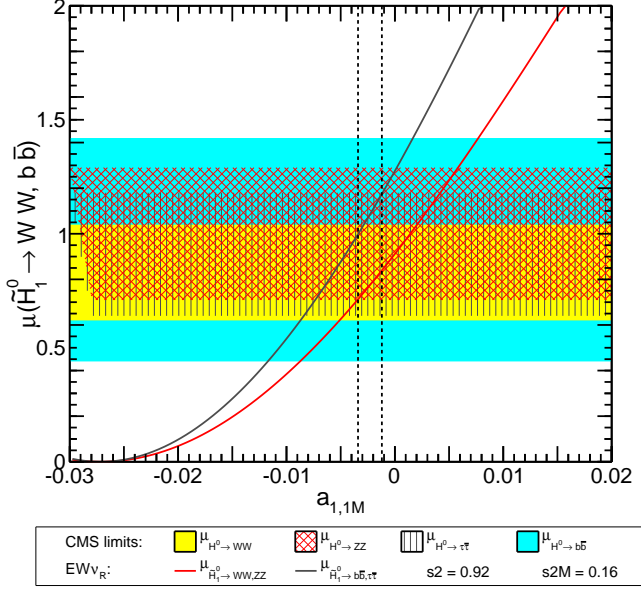


FIG. 11. The graph shows how $\mu(\tilde{H} \rightarrow WW, ZZ)$ and $\mu(\tilde{H} \rightarrow f\bar{f})$ vary with ‘ $a_{1,1M}$ ’. The shaded areas show limits on μ ’s for different channels from data at CMS (refer to Table II). The two leftmost black dashed lines (and two rightmost lines) enclose a range of $a_{1,1M}$ that is consistent with all the constraints analyzed in this paper including those coming from $\tilde{H}' \rightarrow WW$.

within the said ranges, diagonalized the custodial singlet scalar mass matrix in Eq. (A24) and checked if at least one of \tilde{H} , \tilde{H}' , \tilde{H}'' obtains a mass of 125.7 ± 1 GeV - let us denote this state by \tilde{H} , as before. When a combination of these parameters satisfied this condition, we checked if the signal strengths of \tilde{H} in various decay channels agreed with corresponding signal strengths of the 126 GeV Higgs as measured at CMS. To calculate signal strengths for \tilde{H} -decays in $EW\nu_R$ model gluon-gluon fusion production channel was considered, which is the most dominant production channel for the Higgs boson at LHC. When we scanned randomly generated 4 million combinations of these parameters which give at least one 126 GeV scalar particle, we found 1348 combinations for which, the signal strengths of this particle are within 1σ constraints from CMS based on the signal strengths of the 126 GeV Higgs boson at the LHC, in WW , ZZ , $b\bar{b}$, $\tau\bar{\tau}$ and $\gamma\gamma$ decay channels [refer table]. In addition to the parameters in Eq (30) following parameters are required to calculate the partial widths of $\tilde{H} \rightarrow \gamma\gamma$ and $\tilde{H} \rightarrow gg$

and the cross section of $gg \rightarrow \tilde{H}$:

$$0 \leq \lambda_5 \leq 15, \text{ varied with } \Delta\lambda_5 \sim 1.07,$$

$$\lambda_8 = -1, m_{H_3^+} = m_{H_{3M}^+} = 500 \text{ GeV},$$

$$m_{H_5^+} = 200 \text{ GeV}, m_{H_5^{++}} = 320 \text{ GeV}, m_{q_3^M} = 120 \text{ GeV},$$

$$m_{q_1^M} = m_{q_2^M} = m_{l_1^M} = 102 \text{ GeV}. \quad (31)$$

It was found that in most of these 1348 combinations \tilde{H} has H_1^0 as a subdominant component at ~ 126 GeV mass. It can be seen with the help of calculations of signal strengths explained in Appendix B that the branching ratios of such 126 GeV scalar particles are, in general, different from those of a SM-like Higgs. However, the interplay between deviations of their production cross sections and branching ratios (BR) from the corresponding cross sections and BR for a SM-like Higgs, can result in signal strengths close to the SM predictions. Note that in most of these cases H_1^0 , which comes from an SM-like $SU(2)$ scalar doublet, is a dominant component in a mass eigenstate heavier than 126 GeV. Table V lists 29 examples of the 1348 cases, with the masses of \tilde{H} , \tilde{H}' , \tilde{H}'' , their mixing-matrix elements, and signal strengths for various decay channels. For clarity the first row of the table shows the following mixing matrix:

Example 1 (row 1 of Table V):

$$\begin{pmatrix} \tilde{H} \\ \tilde{H}' \\ \tilde{H}'' \end{pmatrix} = \begin{pmatrix} 0.121 & 0.119 & 0.985 \\ 0.918 & 0.364 & -0.157 \\ -0.0378 & 0.924 & -0.065 \end{pmatrix} \begin{pmatrix} H_1^0 \\ H_{1M}^0 \\ H_1^{0'} \end{pmatrix}, \quad (32)$$

with $m_{\tilde{H}} = 125.4$ GeV, $m_{\tilde{H}'} = 580$ GeV, $m_{\tilde{H}''} = 979$ GeV, and $\mu(\tilde{H} \rightarrow W^+W^-/ZZ) = 0.97$, $\mu(\tilde{H} \rightarrow \gamma\gamma) = 0.94$, $\mu(\tilde{H} \rightarrow b\bar{b}/\tau\bar{\tau}) = 1.07$. Thus, in this case

$$\tilde{H} \sim H_1^{0'}, \quad \tilde{H}' \sim H_1^0, \quad \tilde{H}'' \sim H_{1M}^0. \quad (33)$$

Comparison of the signal strengths for three examples from Table V with the CMS measurements for the 126 GeV Higgs boson can be seen in Fig. 12. Eq. (32) shows one of the cases in the figure. The other two are as follows:

Example 2 (row 4 of Table V):

$$\begin{pmatrix} \tilde{H} \\ \tilde{H}' \\ \tilde{H}'' \end{pmatrix} = \begin{pmatrix} 0.173 & 0.081 & 0.982 \\ 0.952 & 0.24 & -0.187 \\ 0.251 & -0.967 & 0.036 \end{pmatrix} \begin{pmatrix} H_1^0 \\ H_{1M}^0 \\ H_1^{0'} \end{pmatrix}, \quad (34)$$

with $\tilde{H} \sim H_1^{0'}$, $\tilde{H}' \sim H_1^0$, $\tilde{H}'' \sim H_{1M}^0$; $m_{\tilde{H}} = 125.4$ GeV, $m_{\tilde{H}'} = 412$ GeV, $m_{\tilde{H}''} = 953$ GeV, and $\mu(\tilde{H} \rightarrow W^+W^-/ZZ) = 0.90$, $\mu(\tilde{H} \rightarrow \gamma\gamma) = 1.20$,

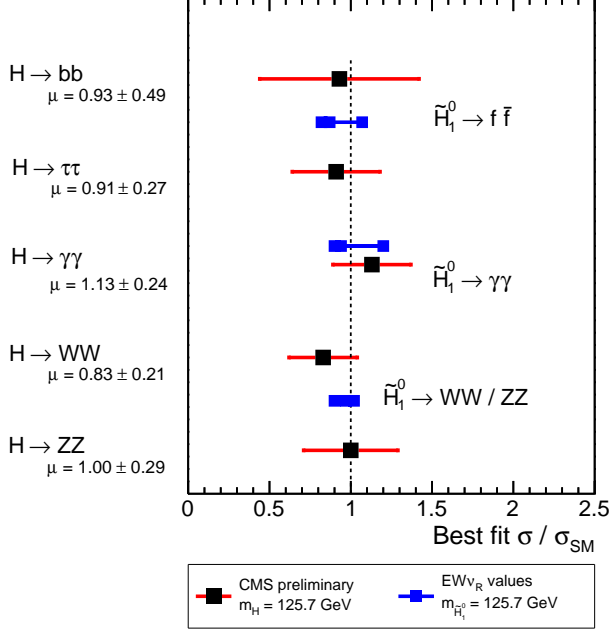


FIG. 12. The figure shows predictions of $\mu(\tilde{H} \rightarrow W^+W^-, ZZ, b\bar{b}, \tau\bar{\tau})$ by $EW\nu_R$ model in $\tilde{H} \sim H_{1M}^0/H_1^{0'}$ scenario for three examples from Table V, in comparison with corresponding best fit values by CMS.

$$\mu(\tilde{H} \rightarrow b\bar{b}/\tau\bar{\tau}) = 0.82.$$

Example 3 (row 11 of Table V):

$$\begin{pmatrix} \tilde{H} \\ \tilde{H}' \\ \tilde{H}'' \end{pmatrix} = \begin{pmatrix} 0.287 & -0.07 & -0.955 \\ 0.224 & -0.965 & 0.138 \\ 0.931 & 0.253 & 0.262 \end{pmatrix} \begin{pmatrix} H_1^0 \\ H_{1M}^0 \\ H_1^{0'} \end{pmatrix}, \quad (35)$$

with $\tilde{H} \sim H_1^{0'}$, $\tilde{H}' \sim H_{1M}^0$, $\tilde{H}'' \sim H_1^0$; $m_{\tilde{H}} = 125.6$ GeV, $m_{\tilde{H}'} = 318$ GeV, $m_{\tilde{H}''} = 1072$ GeV, and $\mu(\tilde{H} \rightarrow W^+W^-/ZZ) = 1.02$, $\mu(\tilde{H} \rightarrow \gamma\gamma) = 0.90$, $\mu(\tilde{H} \rightarrow b\bar{b}/\tau\bar{\tau}) = 0.87$.

This demonstrates that the measurements of the signal strengths do not conclusively indicate that the 126 GeV Higgs boson discovered at LHC is indeed a SM-like Higgs or that it has a dominant SM-like scalar component. As can be seen from Eq (31) we scanned only a part of available parameter space by fixing values or ranges of these parameters. A thorough scan of the entire parameter space is out of scope of this paper. Such a thorough scan or scan of another part of the parameter space could be a topic for a future publication, especially if more data from LHC shows signs of BSM physics. Here we only intended to provide a proof of concept that the 126 GeV SM-lookalike Higgs boson discovered at the

LHC can very well be an impostor with a highly sub-dominant SM-like component in the $EW\nu_R$ model.

In this section we explored two types of scenarios, to study the nature of the SM-lookalike 126 GeV Higgs boson at LHC within the regime of the $EW\nu_R$ model. We showed that this Higgs boson can very well be an impostor with a dual-like nature in the $EW\nu_R$ model. This Higgs boson can show SM-like signal strengths, when it has a dominant SM-like Higgs component. But interestingly, even though it has a highly sub-dominant component of a SM-like Higgs, this Higgs boson can have signal strengths that agree with the data at CMS. Thus, the agreement of the signal strengths of the 126 GeV Higgs at the LHC with the SM-predictions is not sufficient to conclude whether this is the SM-Higgs or a SM-like Higgs impostor or a SM-unlike Higgs impostor!

We showed that in this model the 126 GeV Higgs appears with a dual-like nature. In both the cases signal strengths of this mass eigendiscussed how the 126 GeV Higgs boson at the LHC can be an impostor Higgs within the framework of the $EW\nu_R$ model. The agreement of its signal strengths with the SM-predictions in various decay channels is not sufficient to conclude that this is a SM-Higgs, or that SM-like Higgs is a dominant component in this particle.

TABLE IV. Comparison of production cross-section and branching ratios for various channels in SM and the $\text{EW}\nu_R$ model for row 1 in Table V, also in Eq. (32), where $126 \text{ GeV } \tilde{H} \sim H_1^{0'}$. Note how although the production cross-section and branching ratios for various channels are different in the two models, the product $\sigma \times \text{BR}$ can still be numerically similar.

	SM			$\text{EW}\nu_R$			$\mu = \frac{(\sigma_{Hgg} \times BR)_{\text{SM}}}{(\sigma_{\tilde{H}gg} \times BR)_{\text{EW}\nu_R}}$
	$\Gamma_{H \rightarrow gg}$ $\propto \sigma_{gg \rightarrow H}$	BR	$\Gamma_{Hgg} \times BR$	$\Gamma_{\tilde{H} \rightarrow gg}$ $\propto \sigma_{gg \rightarrow H}$	BR	$\Gamma_{\tilde{H}gg} \times BR$	
$\tilde{H} \rightarrow WW$	3.51E-04	2.21E-01	7.77E-05	5.33E-04	7.55E-01	7.55E-05	0.97
$\tilde{H} \rightarrow ZZ$	3.51E-04	2.74E-02	9.63E-06	5.33E-04	9.36E-02	9.36E-06	0.97
$\tilde{H} \rightarrow bb$	3.51E-04	5.71E-01	2.01E-04	5.33E-04	2.14E-01	2.14E-04	1.07
$\tilde{H} \rightarrow \tau\bar{\tau}$	3.51E-04	6.25E-02	2.20E-05	5.33E-04	4.40E-02	2.34E-05	1.07
$\tilde{H} \rightarrow \gamma\gamma$	3.51E-04	2.28E-03	8.01E-07	5.33E-04	1.41E-03	7.50E-07	0.94

TABLE V. All the masses and the total width of \tilde{H} are given in GeV. Fixed parameters as given in Eq. (31).

s_2	s_{2M}	s_M	λ_1	λ_2	λ_3	λ_4	λ_5	$m_{\tilde{H}}$	$m_{\tilde{H}'}$	$m_{\tilde{H}''}$	$a_{1,1}$	$a_{1,1M}$	$a_{1,1'}$	$a_{1,M,1}$	$a_{1,M,1'}$	$a_{1,1'}$	$a_{1,1M}$	$a_{1,1'}$	$a_{1,1M}$	$a_{1,1'}$	$\Gamma_{\tilde{H}}$	$\mu_{\tilde{H}WW/ZZ}$	$\mu_{\tilde{H}\gamma\gamma}$	$\mu_{\tilde{H}bb/\tau\tau}$
1	0.29	0.94	0.16	12.21	3.68	7.70	-1.69	4.29	125.4	580	979	0.121	0.119	0.985	0.918	-0.157	-0.378	0.924	-0.065	1.34×10^3	0.97	0.94	1.07	
2	0.29	0.94	0.15	12.27	3.85	7.69	-1.69	5.36	125.4	591	1012	0.111	0.106	0.988	0.931	-0.141	-0.347	0.936	-0.061	1.09×10^3	0.83	1.19	0.85	
3	0.3	0.92	0.25	4.55	4.09	2.71	-0.82	12.86	125.4	399	1164	0.163	0.055	0.985	0.982	-0.167	0.091	-0.995	0.041	1.60×10^3	1.02	1.03	1.16	
4	0.46	0.88	0.15	3.04	3.24	6.07	-0.94	5.36	125.4	412	953	0.173	0.081	0.982	0.952	-0.187	0.251	-0.967	0.036	1.08×10^3	0.9	1.2	0.82	
5	0.32	0.93	0.16	8.28	2.54	6.13	-1.12	5.36	125.5	532	827	0.102	0.112	0.988	-0.889	0.141	-0.447	0.893	-0.055	9.87×10^4	1.02	1.27	0.65	
6	0.34	0.93	0.16	5.45	2.94	6.05	-1.08	5.36	125.5	454	909	0.138	0.091	0.986	0.951	-0.158	0.276	-0.96	0.05	1.22×10^3	0.89	1.05	0.97	
7	0.29	0.92	0.27	4.72	3.99	2.43	-0.76	0.00	125.6	392	1155	0.158	0.054	0.986	0.984	-0.161	0.082	-0.996	0.041	1.64×10^3	1.03	0.95	1.14	
8	0.29	0.92	0.27	4.72	3.99	2.43	-0.76	13.93	125.6	392	1155	0.158	0.054	0.986	0.984	-0.161	0.082	-0.996	0.041	1.64×10^3	1.03	0.95	1.14	
9	0.29	0.92	0.27	4.72	3.99	2.43	-0.76	15.00	125.6	392	1155	0.158	0.054	0.986	0.984	-0.161	0.082	-0.996	0.041	1.64×10^3	1.03	1.26	1.13	
10	0.34	0.92	0.21	2.22	1.45	2.71	-0.40	9.64	125.6	304	662	0.157	0.079	0.984	0.972	-0.168	0.176	-0.983	0.051	1.24×10^3	0.88	1.27	0.86	
11	0.9	0.21	0.38	-0.21	5.35	0.91	2.76	1.07	125.6	318	1072	0.287	-0.07	-0.955	0.224	-0.965	0.138	0.931	0.253	1.52×10^3	1.02	0.9	0.87	
12	0.9	0.25	0.37	-0.35	6.07	1.13	3.01	1.07	125.6	401	1114	0.298	-0.074	-0.952	0.298	-0.94	0.167	0.907	0.334	1.06×10^3	0.74	0.94	0.8	
13	0.3	0.93	0.19	7.54	4.66	4.98	-1.35	8.57	125.7	502	1196	0.137	0.069	0.988	0.978	-0.149	0.158	-0.986	0.047	1.27×10^3	0.84	0.94	1	
14	0.3	0.93	0.19	7.54	4.66	4.98	-1.35	9.64	125.7	502	1196	0.137	0.069	0.988	0.978	-0.149	0.158	-0.986	0.047	1.27×10^3	0.84	1.33	1	
15	0.29	0.94	0.19	6.49	3.34	4.06	-0.97	9.64	125.8	451	1017	0.119	0.067	0.991	0.981	-0.128	0.152	-0.987	0.049	1.15×10^3	0.86	1	0.87	
16	0.35	0.92	0.19	3.03	1.86	3.56	-0.56	8.57	125.8	366	743	0.131	0.077	0.988	0.969	-0.144	0.211	-0.976	0.048	9.48×10^4	0.84	1.11	0.65	
17	0.36	0.87	0.35	2.24	4.34	1.38	-0.45	1.07	125.8	332	1194	0.197	0.037	0.98	0.979	-0.198	0.05	-0.998	0.028	1.64×10^3	1.02	1.27	0.72	
18	0.36	0.87	0.35	2.24	4.34	1.38	-0.45	2.14	125.8	332	1194	0.197	0.037	0.98	0.979	-0.198	0.05	-0.998	0.028	1.64×10^3	1.02	0.99	0.72	
19	0.45	0.87	0.18	4.77	4.68	5.98	-1.33	6.43	125.8	530	1145	0.16	0.082	0.984	0.954	-0.175	0.254	-0.966	0.04	1.01×10^3	1	1.14	0.69	
20	0.87	0.25	0.43	-0.12	3.39	0.66	1.94	0.00	125.8	300	897	0.335	-0.069	-0.94	0.272	-0.948	0.166	0.902	0.311	1.19×10^3	0.93	1.04	0.91	
21	0.88	0.25	0.4	-0.18	3.64	0.83	2.36	1.07	125.8	310	993	0.311	-0.08	-0.947	0.271	-0.948	0.169	0.911	0.309	1.43×10^3	0.99	1.27	0.97	
22	0.88	0.2	0.43	-0.18	6.80	0.74	1.93	0.00	125.8	355	883	0.33	-0.053	-0.942	0.246	-0.959	0.14	0.911	0.278	1.03×10^3	0.8	0.99	0.79	
23	0.88	0.22	0.41	-0.19	5.92	0.78	2.01	0.00	125.9	356	906	0.322	-0.056	-0.945	0.266	-0.953	0.147	0.908	0.299	9.74×10^4	0.75	0.91	0.74	
24	0.88	0.17	0.45	-0.21	10.03	0.72	2.39	0.00	125.9	370	977	0.339	-0.048	-0.94	0.202	-0.972	0.123	0.919	0.231	1.14×10^3	0.92	1.12	0.86	
25	0.93	0.21	0.29	-0.35	4.71	1.52	3.37	0.00	125.9	301	1192	0.234	-0.099	-0.967	0.228	-0.961	0.153	0.945	0.256	2.82×10^3	0.74	0.96	0.67	
26	0.93	0.21	0.29	-0.35	4.71	1.52	3.37	5.36	125.9	301	1192	0.234	-0.099	-0.967	0.228	-0.961	0.153	0.945	0.256	2.82×10^3	0.74	1.13	0.67	
27	0.92	0.2	0.33	-0.45	5.20	1.45	3.35	2.14	126	302	1165	0.281	-0.141	-0.949	0.209	-0.957	0.204	0.937	0.255	6.23×10^3	0.89	1.08	1.04	
28	0.94	0.18	0.3	-0.42	7.37	1.57	2.87	5.36	126	322	1076	0.246	-0.093	-0.965	0.204	-0.968	0.145	0.948	0.232	3.47×10^3	0.73	0.96	0.75	
29	0.94	0.15	0.32	-0.53	9.80	1.61	3.41	2.14	126	322	1162	0.258	-0.105	-0.961	0.167	-0.974	0.151	0.952	0.199	6.08×10^3	0.81	1.36	0.85	

VI. SIGNALS OF CP-ODD SPIN ZERO STATES

So far in this model, the 126 GeV Standard Model like BEH boson is most likely \tilde{H}_1^0 . There are also, CP-odd spin zero states, H_3^0, H_{3M}^0 , and the other heavy CP-even spin zero states, H_{1M}^0 , and \tilde{H}'_1 . In this section, we show possibilities to probe the signal of these pseudo-scalars in various major channels at LHC. To do so, we will investigate the product of cross section production and branching ratio, a.k.a signal strength, in $\gamma\gamma$ and $\tau\tau$ channels. And also, we will calculate the ratio of signal strength μ , defined below, between these pseudo-scalars and a Standard Model like Higgs boson H_{sm} in other channels.

$$\mu = \frac{\sigma(gg \rightarrow H_{3,3M}^0) Br(H_{3,3M}^0 \rightarrow XX)}{\sigma(gg \rightarrow H_{sm}) Br(H_{sm} \rightarrow XX)} \quad (36)$$

In this extension of EW ν_R model, the degenerate masses of two $SU(2)_D$ custodial triplets are related by:

$$\frac{m_{H_3}^2}{m_{H_{3M}}^2} = \frac{1}{1 + \cos\theta_M^2} \quad (37)$$

Assuming that neutral states, H_3^0 and H_{3M}^0 , obey this relationship. And, here we use two cases of $\sin\theta_M = 0.4; 0.87$. The lighter one, $m_{H_3^0}$, is scanned from 130 – 460 GeV and 130 – 540 GeV, then the heavier one, $m_{H_{3M}^0} = 176 – 610$ GeV and 145 – 601 GeV, respectively.

A. Ratio of production cross section

At LHC, H_3^0, H_{3M}^0 are produced mainly via gluon fusion similar to H_{sm} . By using effective coupling approximation, we have

$$R = \frac{\sigma(gg \rightarrow H_{3,3M}^0)}{\sigma(gg \rightarrow H_{sm})} \approx \frac{\Gamma(H_{3,3M}^0 \rightarrow gg)}{\Gamma(H_{sm} \rightarrow gg)} \quad (38)$$

Gluonic decay of H_{sm} is formulated in [AK's part]. H_3^0 does not couple directly to vector boson, W, Z . And triplet couplings, such as $H_3^0 H_3^+ H_3^-$, $H_3^0 H_5^+ H_5^-$, $H_3^0 H_5^{++} H_5^{--}$, are forbidden by CP conservation. Then, only fermionic loops from quarks, top quark and mirror quarks, contribute to gluonic decay of H_3^0 and H_{3M}^0 [20]

$$\Gamma(H_{3,3M}^0 \rightarrow gg) = \frac{G_F \alpha_s^2}{16\sqrt{2}\pi^3} m_{H_{3,3M}^0}^3 \left| \sum_Q g_Q^{H_{3,3M}^0} F_Q^{H_{3,3M}^0}(\tau_f) \right|^2 \quad (39)$$

$$F_Q^{H_{3,3M}^0}(\tau_f) = \tau_f f(\tau_f); \quad (40)$$

$$\tau_t = 4m_f^2/m_{H_{3,3M}^0}^2 \quad (41)$$

$g_Q^{H_{3,3M}^0}$ are couplings of H_3^0 and H_{3M}^0 to top quark and mirror quarks, listed in [coupling table].

Here, \sum_Q is summed over top quark and mirror quarks. However, the contributions from mirror quarks can be suppressed due to the fact that mirror up quarks and mirror down quarks couple to H_3^0, H_{3M}^0 in opposite ways. Particularly, in this work, we consider degenerate mirror fermion doublets, means $m_{u^M} = m_{d^M}$, then contributions from mirror quarks are canceled out. So, only loop from top quark appears in the production of H_3^0, H_{3M}^0 . Then, the ratios of production cross section are:

$$R_{H_3^0} = \tau_t^2 \left| \frac{\tan\theta_M f(\tau_t)}{\tau_t + (\tau_t - 1)f(\tau_t)} \right|^2 \quad (42)$$

For H_3^0

$$R_{H_{3M}^0} = \tau_t^2 \left| \frac{\sin\theta_M f(\tau_t)}{\sin\theta_2(\tau_t + (\tau_t - 1)f(\tau_t))} \right|^2 \quad (43)$$

For H_{3M}^0

B. In $\gamma\gamma$ channel

ATLAS [21] and CMS [22] have recently reported their results in searching for narrow scalar diphoton resonances up to 600 GeV for CMS and 840 GeV for ATLAS. In those reports, they present the upper limit on the production cross section times branching ratio into two photons at 95% confidence level. So far, no significant excess has been found, except two ones with a 2σ above the background at $m = 201$ GeV and $m = 530$ GeV in the ATLAS analysis. Subjectively, we compare our prediction in $\gamma\gamma$ channel with those results, even though assumptions about decay width of the resonance are made in those reports.

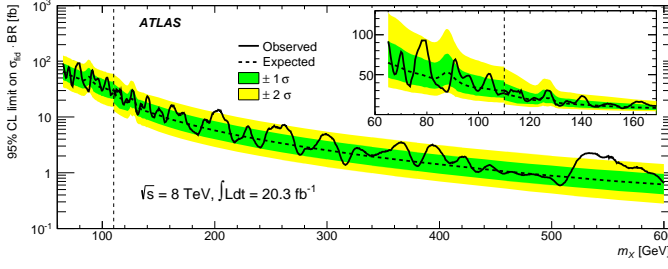


FIG. 13. ATLAS's 95% confidence level limit on the production cross section times branching ratio $BR(X \rightarrow \gamma\gamma)$ as a function of m_X

Similar to the gluonic decay, only fermionic loops contribute to the partial width of $H_{3,3M}^0 \rightarrow \gamma\gamma$, [20]

$$\Gamma(H_{3,3M}^0 \rightarrow \gamma\gamma) = \frac{g^2 \alpha^2 m_{H_{3,3M}^0}^3}{256 \pi m_W^2} \left| \sum_i N_{ci} e_i^2 g_i F_i^{H_{3,3M}^0} \right|^2. \quad (44)$$

Here, i = top quark, six mirror quarks, and three mirror charged leptons. While the total widths of $H_{3,3M}^0$ are calculated by summing all partial widths.

$$\begin{aligned} \Gamma_{H3,H3M} &= \Gamma(H_{3,3M}^0 \rightarrow \gamma\gamma) + \Gamma(H_{3,3M}^0 \rightarrow gg) \\ &+ \Gamma(H_{3,3M}^0 \rightarrow W^+W^-) + \Gamma(H_{3,3M}^0 \rightarrow ZZ) \\ &+ \Gamma(H_{3,3M}^0 \rightarrow \tau\bar{\tau}) + \Gamma(H_{3,3M}^0 \rightarrow t\bar{t}) \\ &+ \Gamma(H_{3,3M}^0 \rightarrow c\bar{c}) + \Gamma(H_{3,3M}^0 \rightarrow b\bar{b}) \\ &+ \sum_{i=1}^6 \Gamma(H_{3,3M}^0 \rightarrow q_M^i \bar{q}_M^i) \\ &+ \sum_{j=1}^3 \Gamma(H_{3,3M}^0 \rightarrow l_M^j \bar{l}_M^j) \end{aligned} \quad (45)$$

The branching ratio of $H_{3,3M}^0 \rightarrow \gamma\gamma$ is

$$Br(H_{3,3M}^0 \rightarrow \gamma\gamma) = \frac{\Gamma(H_{3,3M}^0 \rightarrow \gamma\gamma)}{\Gamma_{H3,H3M}} \quad (46)$$

The signal strength of $H_{3,3M}^0 \rightarrow \gamma\gamma$ is defined as

$$\begin{aligned} \sigma \cdot Br(H_{3,3M}^0 \rightarrow \gamma\gamma) &= R \times \sigma(gg \rightarrow H_{sm}) \\ &\times Br(H_{3,3M}^0 \rightarrow \gamma\gamma) \end{aligned}$$

At any particular mass, ratio of production cross section R , and $Br(H_{3,3M}^0 \rightarrow \gamma\gamma)$ is calculated directly. While $\sigma(gg \rightarrow H_{sm})$ is taken from the handbook of Higgs cross section [24]. To be consistent with previous

analysis, we also provide two scenarios which correspond to the dual nature of the 125-GeV Higgs impostor. And for illustrating, we consider the degenerate case in masses of mirror fermions. Particularly, the first two generations of mirror quarks and all charged leptons have same masses, $m_{q_1^M} = m_{q_2^M} = m_{l^M} = 102$ GeV. All right-handed neutrinos' masses are at $M_R = 75$ GeV. One mixing angle in doublet scalars is fixed, $\theta_2 = 0.3$.

- In the case of H_1^0 being dominant in the mixing state \tilde{H}_1^0 , the heaviest mirror quarks are $m_{q_3^M} = 120$ GeV, the mixing angles $\sin\theta_M = 0.4$, $\sin\theta_{2M} = 0.86$

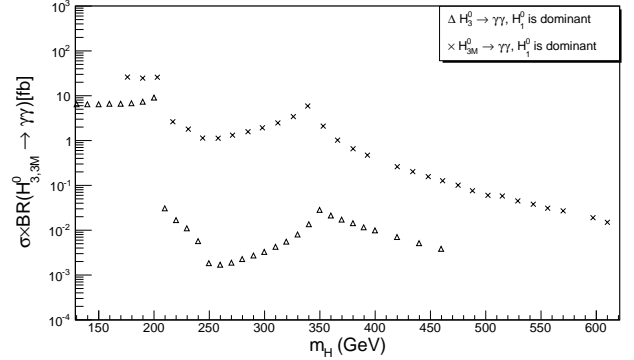


FIG. 14. The production cross section times branching ratio in $\gamma\gamma$ channel of H_3^0 and H_{3M}^0 . $m_{H_3^0} = 130 - 460$ GeV, $m_{H_{3M}^0} = 145 - 602$ GeV

- While in the other case when H_1^0 is sub-dominant, a set of parameters is choose as $m_{q_3^M} = 173$ GeV, $\sin\theta_M = 0.87$, and $\sin\theta_{2M} = 0.39$.

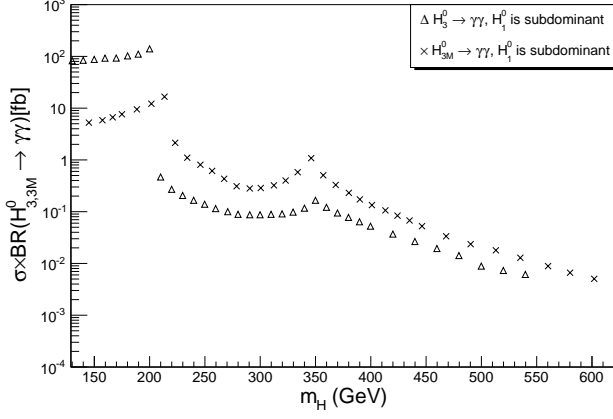


FIG. 15. The production cross section times branching ratio in $\gamma\gamma$ channel of H_3^0 and H_{3M}^0 . $m_{H_3^0} = 130 - 540$ GeV, $m_{H_{3M}^0} = 176 - 610$ GeV

Remark:

- Before fermionic thresholds, $2m_{q_{1,2}^M}$, $2m_{lM}$, the signal strength can be larger than what ATLAS and CMS represent. To be conservative, we can exclude a range of mass of pseudo-scalars corresponding to two examples of parameter set above. However, with different set up, the signal strength could be well below.
- As $m_{H_3^0}$ increasing, more mirror fermionic decay channels are opened up. The branching ratios of $H_{3,3M} \rightarrow \gamma\gamma$ peaks at thresholds, $2m_{q_{1,2}^M}$, $2m_{q_3^M}$, $2m_{lM}$, $2m_t$. And production cross section decreases. So both signal strengths are below the limit.

C. In $\tau\tau$ channel

Recently, ATLAS [25] and CMS [26] also reported their new results in $\tau\tau$ channel. Although, the main aim of their reports are to look for MSSM neutral boson, they provide a model independent limit on the production cross section times branching ratio of a general spin zero state. Therefore, in this part, we investigate the signal strength of our $H_{3,3M}^0 \rightarrow \tau\tau$ in two sets of parameters, when H_1^0 is either dominant or sub-dominant in \tilde{H}_1^0 , as the same with what we did in the last part.

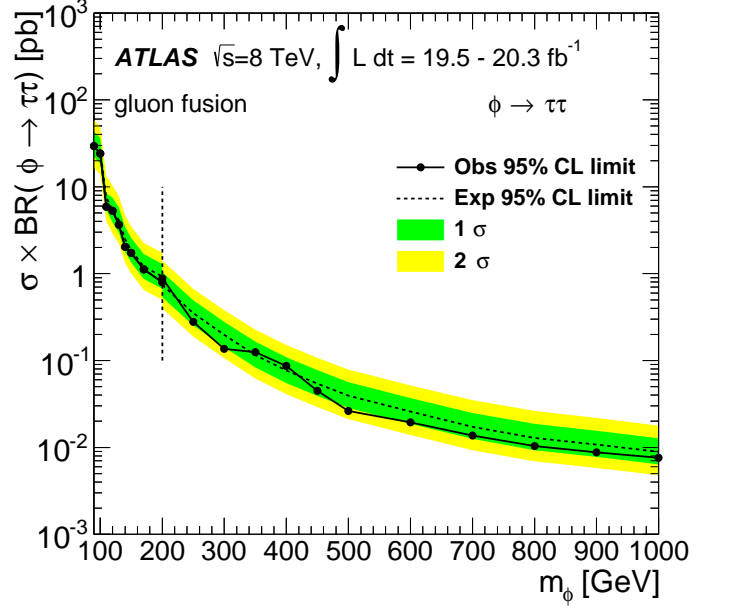


FIG. 16. ATLAS's 95% CL upper limits on the cross section of a scalar boson produced via gluon fusion times the branching fraction into τ pairs

- When H_1^0 is dominant.

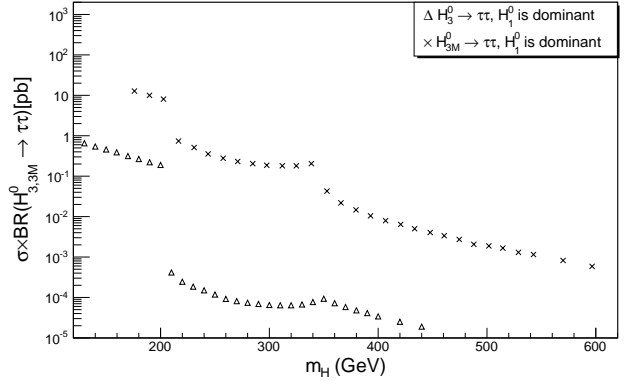


FIG. 17. The production cross section times branching ratio in $\tau\tau$ channel of H_3^0 and H_{3M}^0 . $m_{H_3^0} = 130 - 460$ GeV, $m_{H_{3M}^0} = 145 - 602$ GeV

- When H_1^0 is sub-dominant.

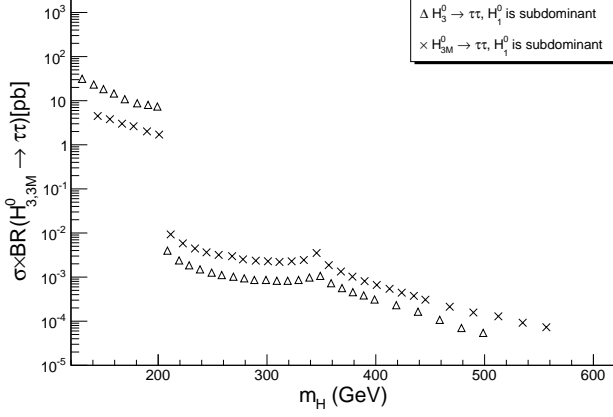


FIG. 18. The production cross section times branching ratio in $\tau\tau$ channel of H_3^0 and H_{3M}^0 . $m_{H_3^0} = 130 - 540$ GeV, $m_{H_{3M}^0} = 176 - 610$ GeV

Remark:

- In both cases, the signal strength can exceed the upper limit from ATLAS and CMS before the thresholds of mirror fermions, here is 204 GeV. It happens because unlike SM Higgs, the decaying processes such as $H_{3,3M}^0 \rightarrow WW/ZZ$ only happen at loop level. So the partial widths of those are relatively small. Consequently, the branching ratios of $H_{3,3M} \rightarrow \tau\bar{\tau}$ are not as small as in Standard Model. Even though, they are at one order above the limit. And in the wide range of parameter space in the $EW\nu_R$ model, it is not a problematic to fit the model into the upcoming analyses at LHC in this mass region.
- After passing the first threshold, the signal strengths of both $H_{3,3M} \rightarrow \tau\bar{\tau}$ decrease rapidly, because the total widths $\Gamma_{H_{3,3M}}$ are dominated by fermionic decays. And, then they reach another peak at $2m_t$. In the whole region, the signal strengths are below the limit for both pseudo-scalars. Except, at around $2m_t$, the signal strength can be slightly above the limit. For example, in case H_1^0 being dominant, and at $m_H = 340$ GeV, $\sigma \times BR(H_{3M}^0 \rightarrow \tau\bar{\tau}) = 0.18$, while $\sigma \times BR(H_{sm} \rightarrow \tau\bar{\tau}) = 0.12$. It is justifiable.

D. In WW/ZZ channels

In this model, pseudo-scalars, H_3^0, H_{3M}^0 do not couple directly to W , and Z . Decay processes $H_{3,3M}^0 \rightarrow WW/ZZ$ happen only at loop levels. It is predictable that these processes will be highly suppressed. To prove that, we calculate the ratio of signal strength, μ , between $H_3^0 \rightarrow WW/ZZ$ and $H_{sm} \rightarrow WW/ZZ$. μ is defined in Eq (??).

$$\mu^{VV} = \frac{\sigma(gg \rightarrow H_3^0) Br(H_3^0 \rightarrow VV)}{\sigma(gg \rightarrow H_{sm}) Br(H_{sm} \rightarrow VV)}$$

$$= R_{H_3^0} \frac{Br(H_3^0 \rightarrow VV)}{Br(H_{sm} \rightarrow VV)} \quad (47)$$

Here $V = W, Z$. At any particular mass, $Br(H_{sm} \rightarrow VV)$ is taken from the handbook of Higgs working group [24]. While the ratio of production cross section $R_{H_3^0}$ (??) and $Br(H_3^0 \rightarrow VV)$ are calculated directly. At one loop order, the partial decay rate for these processes are [27]

- $H_3^0 \rightarrow WW$

$$\Gamma(H_3^0 \rightarrow WW) = \frac{3^2 g^6 (m_{H_3^0}^2 - 4m_W^2)^{3/2}}{2^{14} \pi^5 m_W^2} |A_{WW}|^2 \quad (48)$$

$$A_{WW} = m_t^2 t_M A_t^W - m_b^2 t_M^2 A_b^W + \frac{m_{lM}^2}{\sqrt{2}} A_{lM}^W + \frac{M_R^2}{\sqrt{2} c_M} A_{\nu R}^W \quad (49)$$

- $H_3^0 \rightarrow ZZ$

$$\Gamma(H_3^0 \rightarrow ZZ) = \frac{3^2 g^6 (m_{H_3^0}^2 - 4m_Z^2)^{3/2}}{2^{15} \pi^5 m_W^2} |A_{ZZ}|^2 \quad (50)$$

$$A_{ZZ} = m_t^2 t_M A_t^Z - m_b^2 t_M A_b^Z + \frac{m_{lM}^2}{\sqrt{2}} A_{lM}^Z \quad (51)$$

$A_f^{W/Z}$ are amplitudes with top, bottom quarks; mirror charged leptons, and right handed neutrinos inside the loops.

They have specific forms in the Appendix ??.

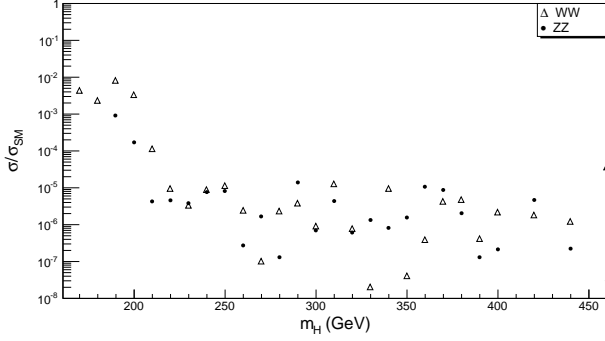


FIG. 19. Ratio of strength signal in WW/ZZ channel of H_3^0 comparing to H_{sm}

As it is predicted, the signal strengths of H_3^0 in vector boson channels are heavily suppressed.

$$\text{E. } (H_3^0 \rightarrow \bar{l}^M l^M)/(H_{sm} \rightarrow WW)$$

At LHC, $H \rightarrow WW$ is an important channel to probe new scalars in the high mass region. From Fig. ??, we see that the ratio of signal strength is suppressed very much for CP-odd scalar, H_3^0 , in this model. However, it can be detected via a two state decay process: $H_3^0 \rightarrow \bar{l}^M l^M \rightarrow \bar{l} \phi_S l \phi_S$, which mimics WW signal of the SM Higgs boson: $H \rightarrow W^+ W^- \rightarrow \bar{l} \nu l \nu$. Here, ϕ_S is invisible, and considered as E_T^M . With a particular set of parameter phase in this work, all charged mirror leptons $m_{l^M} = 102 \text{ GeV}$, $m_H = 210 - 500 \text{ GeV}$, it is sufficient to have both mirror fermions being on-shell.

$$\Gamma(H_3^0 \rightarrow \bar{l}^M l^M) = \frac{g^2 m_{H_3^0}^3 t_M^2}{256\pi m_W^2} \tau_{l^M} \sqrt{1 - \tau_{l^M}} \quad (52)$$

$$\text{Here, } \tau_{l^M} = \frac{4m_{l^M}^2}{m_{H_3^0}^2}$$

$$\Gamma(l^M \rightarrow l \phi_S) = g_{sl}^2 \frac{m_{l^M}}{32\pi} \quad (53)$$

In analogy to previous comparisons, we define a ratio of signal strength:

$$\mu^l = R_{H_3^0} \frac{Br(H_3^0 \rightarrow \bar{l}^M l^M) Br(l^M \rightarrow l \phi_S)}{Br(H \rightarrow W^+ W^-) Br(W \rightarrow l \nu)} \quad (54)$$

With $M_R = 70 \text{ GeV}$, then $l^M \rightarrow \nu_R \nu l$ is kinametically possible.

$$Br(l^M \rightarrow l \phi_S) = \frac{\Gamma(l^M \rightarrow l \phi_S)}{\Gamma(l^M \rightarrow l \phi_S) + \Gamma(l^M \rightarrow \nu_R \nu l)} \quad (55)$$

While $Br(W \rightarrow l \nu) = 0.108$ [28]. It is clear that the ratio μ^l depends on the value of g_{sl} . The search for high-mass Higgs boson in $H \rightarrow WW \rightarrow l \nu l \nu$ was carried on at both ATLAS in the range of 260 – 1000 GeV [29], and CMS in the range of 145 – 1000 GeV [30]. There is no excess in the whole scanning mass region. The observed 95% CL upper limit on the ratio of signal strength is below $\mu = 1$ all the way up to $m_H \approx 600 \text{ GeV}$ in [30]. We can set an upper limit on μ^l , $\mu^l \leq 1$. Consequently, we can have a rough upper limit on g_{sl} , $g_{sl} \leq 10^{-3}$.

VII. CONCLUSIONS

The 126-GeV object has presented us with a challenge to understand its nature: Is it really the SM Higgs boson as it appears to be or is it simply an *impostor*? So far, the only data available to us are given in terms of the so-called signal strengths, μ , as defined in Eq. (??). The signal strengths for the various decay modes of the SM Higgs boson are consistent with data. However, It turns out that it might be possible for various BSM models to be consistent with experiment also based solely on such signal strengths. This is what we have shown in this paper in the context of the $EW\nu_R$ in its extended version.

As we have described in the beginning of our paper, the $EW\nu_R$ [4] was invented with the purpose of realizing the seesaw mechanism at the electroweak scale instead of some GUT scale. As such one can *directly* test the seesaw mechanism at the LHC and at the proposed ILC through the physics associated with the model such as lepton-number violating production of electroweak-scale Majorana right-handed neutrinos and -this is the subject of the present paper- Higgs physics beyond that of the SM.

The extended $EW\nu_R$ model discussed in this paper contains three neutral CP-even mass eigenstates, \tilde{H} , \tilde{H}' and \tilde{H}'' , which are linear combinations of H_1^0 , H_{1M}^0 which couple to SM fermions and mirror fermions respectively and $H_1^{0'}$ which couples only to ν_R 's. The notation for the mass eigenstates \tilde{H} , \tilde{H}' and \tilde{H}'' refers to states with increasing masses. We scanned the parameter space with the following requirements in mind: 1) The mass of the lightest state should be $\sim 126 \text{ GeV}$; 2) The mixing angles should be such that the signal strengths fit the data from CMS and ATLAS. We found many combinations of H_1^0 , H_{1M}^0 and $H_1^{0'}$ which satisfy those requirements.

What is interesting here is the dual nature of the 126-GeV scalar that we uncovered in our scanning of the parameter space: 1) There are states with the SM-like scalar H_1^0 as a dominant component; 2) There are states with $H_1^{0'}$ as a dominant component and is thus *very unlike* that of the SM model. In other words, these states are impostors. All of these states- and we are far from exhausting the parameter space- yield signal strengths compatible with the CMS and ATLAS data.

It goes without saying that detailed studies of various properties of the 126-GeV SM-like scalar such as the total width, partial widths,..., are needed to determine if it were indeed the SM Higgs boson or just simply an *impostor*. Of course, a discovery of one or several extra scalars definitely points toward physics beyond the SM. In the extended $EW\nu_R$ model, although the aforementioned 126-GeV-like scalars all yield comparable signal strengths, details such as production cross sections, branching ratios, total widths and partial widths can differ quite a bit from one another. States with H_1^0 as a dominant component tend to behave more like the SM Higgs boson while *others do not*. In other words, we may have discovered a scalar which is involved in the electroweak symmetry breaking but which *may not be* the SM Higgs boson.

VIII. ACKNOWLEDGEMENTS

We would like to thank Giuseppe Cerati for providing results of the search for SM-like heavy Higgs boson at CMS. This work was supported by US DOE grant DE-FG02-97ER41027. ASK was supported by the Graduate Fellowship of the Department of Physics, University of Virginia.

Appendix A: Scalar Potential and Physical Scalar States in the Extended $EW\nu_R$ Model

When a $Y = 1$ complex scalar doublet is added to the minimal $EW\nu_R$ model, under the global $SU(2)_L \times SU(2)_R$ we have

$$\Phi_2 = \begin{pmatrix} \phi_2^{0,*} & \phi_2^+ \\ \phi_2^- & \phi_2^0 \end{pmatrix}, \quad (\text{A1})$$

$$\Phi_{2M} = \begin{pmatrix} \phi_{2M}^{0,*} & \phi_{2M}^+ \\ \phi_{2M}^- & \phi_{2M}^0 \end{pmatrix}. \quad (\text{A2})$$

and

$$\chi = \begin{pmatrix} \chi^0 & \xi^+ & \chi^{++} \\ \chi^- & \xi^0 & \chi^+ \\ \chi^{--} & \xi^- & \chi^{0*} \end{pmatrix}. \quad (\text{A3})$$

Proper vacuum alignment for $SU(2)_L \times U(1)_Y \rightarrow U(1)_{em}$ gives

$$\langle \Phi_2 \rangle = \begin{pmatrix} v_2/\sqrt{2} & 0 \\ 0 & v_2/\sqrt{2} \end{pmatrix}, \quad (\text{A4})$$

$$\langle \Phi_{2M} \rangle = \begin{pmatrix} v_{2M}/\sqrt{2} & 0 \\ 0 & v_{2M}/\sqrt{2} \end{pmatrix}, \quad (\text{A5})$$

and

$$\langle \chi \rangle = \begin{pmatrix} v_M & 0 & 0 \\ 0 & v_M & 0 \\ 0 & 0 & v_M \end{pmatrix}, \quad (\text{A6})$$

Thus, the VEVs of real parts of Φ_2 , Φ_{2M} and χ are $(v_2/\sqrt{2})$, $(v_{2M}/\sqrt{2})$ and v_M respectively such that

$$v_2^2 + v_{2M}^2 + 8v_M^2 = v^2, \quad (\text{A7})$$

where $v \approx 246$ GeV. We define

$$s_2 = \frac{v_2}{v}; \quad s_{2M} = \frac{v_{2M}}{v}; \quad s_M = \frac{2\sqrt{2}v_M}{v}. \quad (\text{A8})$$

This extension of the $EW\nu_R$ model also has an additional $U(1)_{SM} \times U(1)_{MF}$ global symmetry such that

$$U(1)_{SM} : \Phi_2 \rightarrow e^{i\alpha_{SM}} \Phi_2 \quad (\text{A9})$$

$$l_L^{SM} \rightarrow e^{i\alpha_{SM}} l_L^{SM}, \quad (\text{A10})$$

and

$$U(1)_{MF} : \Phi_{2M} \rightarrow e^{i\alpha_{MF}} \Phi_{2M} \quad (\text{A11})$$

$$l_R^M \rightarrow e^{i\alpha_{MF}} l_R^M. \quad (\text{A12})$$

Also under $U(1)_{SM} \times U(1)_{MF}$

$$\phi_S \rightarrow e^{-i(\alpha_{MF} - \alpha_{SM})} \phi_S, \quad (\text{A13})$$

and all the other fields are singlets under this symmetry.

A generic $SU(2)_L \times SU(2)_R$ preserving potential for these scalars can now be written as

$$\begin{aligned}
V(\Phi_2, \Phi_{2M}, \chi) &= \lambda_1 \left[\text{Tr} \Phi_2^\dagger \Phi_2 - v_2^2 \right]^2 + \lambda_2 \left[\text{Tr} \Phi_{2M}^\dagger \Phi_{2M} - v_{2M}^2 \right]^2 + \lambda_3 \left[\text{Tr} \chi^\dagger \chi - 3v_M^2 \right]^2 \\
&+ \lambda_4 \left[\text{Tr} \Phi_2^\dagger \Phi_2 - v_2^2 + \text{Tr} \Phi_{2M}^\dagger \Phi_{2M} - v_{2M}^2 + \text{Tr} \chi^\dagger \chi - 3v_M^2 \right]^2 \\
&+ \lambda_5 \left[(\text{Tr} \Phi_2^\dagger \Phi_2) (\text{Tr} \chi^\dagger \chi) - 2 (\text{Tr} \Phi_2^\dagger \frac{\tau^a}{2} \Phi_2 \frac{\tau^b}{2}) (\text{Tr} \chi^\dagger T^a \chi T^b) \right] \\
&+ \lambda_6 \left[(\text{Tr} \Phi_{2M}^\dagger \Phi_{2M}) (\text{Tr} \chi^\dagger \chi) - 2 (\text{Tr} \Phi_{2M}^\dagger \frac{\tau^a}{2} \Phi_{2M} \frac{\tau^b}{2}) (\text{Tr} \chi^\dagger T^a \chi T^b) \right] \\
&+ \lambda_7 \left[(\text{Tr} \Phi_2^\dagger \Phi_2) (\text{Tr} \Phi_{2M}^\dagger \Phi_{2M}) - (\text{Tr} \Phi_2^\dagger \Phi_{2M}) (\text{Tr} \Phi_{2M}^\dagger \Phi_2) \right] + \lambda_8 \left[3 \text{Tr} \chi^\dagger \chi \chi^\dagger \chi - (\text{Tr} \chi^\dagger \chi)^2 \right]
\end{aligned} \tag{A14}$$

Note that this potential, like the one in the minimal EW ν_R model is also invariant under $\chi \rightarrow -\chi$. Now it is also invariant under the global $U(1)_{\text{SM}} \times U(1)_{\text{MF}}$ symmetry. The vacuum alignment given above breaks the global $SU(2)_L \times SU(2)_R$ down to the custodial $SU(2)_D$. One still has $M_W = gv/2$ and $M_Z = M_W/\cos\theta_W$, but

now $v = \sqrt{v_2^2 + v_{2M}^2 + 8v_M^2} \approx 246 \text{ GeV}$. It is found that three ‘massless’ Nambu-Goldstone Bosons can be obtained after spontaneous breaking of $SU(2)_L \times U(1)_Y$ to $U(1)_{em}$, when a condition $\lambda_5 = \lambda_6 = \lambda_7$ imposed on the potential above. Thus, the potential that should be used to find the physical Higgs states is

$$\begin{aligned}
V(\Phi_2, \Phi_{2M}, \chi) &= \lambda_1 \left[\text{Tr} \Phi_2^\dagger \Phi_2 - v_2^2 \right]^2 + \lambda_2 \left[\text{Tr} \Phi_{2M}^\dagger \Phi_{2M} - v_{2M}^2 \right]^2 + \lambda_3 \left[\text{Tr} \chi^\dagger \chi - 3v_M^2 \right]^2 \\
&+ \lambda_4 \left[\text{Tr} \Phi_2^\dagger \Phi_2 - v_2^2 + \text{Tr} \Phi_{2M}^\dagger \Phi_{2M} - v_{2M}^2 + \text{Tr} \chi^\dagger \chi - 3v_M^2 \right]^2 \\
&+ \lambda_5 \left[(\text{Tr} \Phi_2^\dagger \Phi_2) (\text{Tr} \chi^\dagger \chi) - 2 (\text{Tr} \Phi_2^\dagger \frac{\tau^a}{2} \Phi_2 \frac{\tau^b}{2}) (\text{Tr} \chi^\dagger T^a \chi T^b) + (\text{Tr} \Phi_{2M}^\dagger \Phi_{2M}) (\text{Tr} \chi^\dagger \chi) \right. \\
&- 2 (\text{Tr} \Phi_{2M}^\dagger \frac{\tau^a}{2} \Phi_{2M} \frac{\tau^b}{2}) (\text{Tr} \chi^\dagger T^a \chi T^b) + (\text{Tr} \Phi_2^\dagger \Phi_2) (\text{Tr} \Phi_{2M}^\dagger \Phi_{2M}) - (\text{Tr} \Phi_2^\dagger \Phi_{2M}) (\text{Tr} \Phi_{2M}^\dagger \Phi_2) \left. \right] \\
&+ \lambda_8 \left[3 \text{Tr} \chi^\dagger \chi \chi^\dagger \chi - (\text{Tr} \chi^\dagger \chi)^2 \right]
\end{aligned} \tag{A15}$$

After the spontaneous breaking of $SU(2)_L \times U(1)_Y \rightarrow U(1)_{em}$, besides the three Nambu-Goldstone Bosons, there are *twelve* physical scalars grouped into $5 + 3 + 3 + 1$ of the custodial $SU(2)_D$ with 3 custodial singlets. To express the Nambu-Goldstone Bosons and the physical scalars let us adopt the following

convenient notation:

$$\begin{aligned}
v &= \sqrt{v_2^2 + v_{2M}^2 + 8v_M^2} \\
s_2 &= \frac{v_2}{v}, \quad s_{2M} = \frac{v_{2M}}{v}, \quad s_M = \frac{2\sqrt{2} v_M}{v}, \\
c_2 &= \frac{\sqrt{v_{2M}^2 + 8v_M^2}}{v}, \quad c_{2M} = \frac{\sqrt{v_2^2 + 8v_M^2}}{v}, \\
c_M &= \frac{\sqrt{v_2^2 + v_{2M}^2}}{v}.
\end{aligned} \tag{A16}$$

Thus,

$$s_2^2 + c_2^2 = s_{2M}^2 + c_{2M}^2 = s_M^2 + c_M^2 = 1. \tag{A17}$$

[In the limit $s_{2M} \rightarrow 0$ i.e. EW $\nu_R^{U(1)_{\text{SM}} \times U(1)_{\text{MF}}} \rightarrow \text{EW}\nu_R$,

$s_M \rightarrow s_H$ and $c_M \rightarrow c_H$]. Let us also define, like we did for the minimal EW ν_R model,

$$\begin{aligned}\phi_2^0 &\equiv \frac{1}{\sqrt{2}} \left(v_2 + \phi_2^{0r} + \imath \phi_2^{0\imath} \right), \\ \phi_{2M}^0 &\equiv \frac{1}{\sqrt{2}} \left(v_{2M} + \phi_{2M}^{0r} + \imath \phi_{2M}^{0\imath} \right), \\ \chi^0 &\equiv v_M + \frac{1}{\sqrt{2}} \left(\chi^{0r} + \imath \chi^{0\imath} \right); \quad (\text{A18})\end{aligned}$$

$$\psi^\pm \equiv \frac{1}{\sqrt{2}} \left(\chi^\pm + \xi^\pm \right), \quad \zeta^\pm \equiv \frac{1}{\sqrt{2}} \left(\chi^\pm - \xi^\pm \right) \quad (\text{A19})$$

for the complex neutral and charged fields respectively. With these fields the Nambu-Goldstone Bosons are given by

$$\begin{aligned}G_3^\pm &= s_2 \phi_2^\pm + s_{2M} \phi_{2M}^\pm + s_M \psi^\pm, \\ G_3^0 &= \imath \left(-s_2 \phi_2^{0\imath} - s_{2M} \phi_{2M}^{0\imath} + s_M \chi^{0\imath} \right). \quad (\text{A20})\end{aligned}$$

The physical scalars can be grouped, as stated in the previous section, based on their transformation properties under $SU(2)_D$ as follows:

$$\begin{aligned}\text{five-plet (quintet)} &\rightarrow H_5^{\pm\pm}, H_5^\pm, H_5^0; \\ \text{triplet} &\rightarrow H_3^\pm, H_3^0; \\ \text{triplet} &\rightarrow H_{3M}^\pm, H_{3M}^0; \\ \text{three singlets} &\rightarrow H_1^0, H_{1M}^0, H_1^{0'} \quad (\text{A21})\end{aligned}$$

where

$$\begin{aligned}H_5^{++} &= \chi^{++}, \quad H_5^+ = \zeta^+, \quad H_5^0 = \frac{1}{\sqrt{6}} \left(2\xi^0 - \sqrt{2}\chi^{0r} \right), \\ H_3^+ &= -\frac{s_2 s_M}{c_M} \phi_2^+ - \frac{s_{2M} s_M}{c_M} \phi_{2M}^+ + c_M \psi^+, \\ H_3^0 &= \imath \left(\frac{s_2 s_M}{c_M} \phi_2^{0\imath} + \frac{s_{2M} s_M}{c_M} \phi_{2M}^{0\imath} + c_M \chi^{0\imath} \right), \\ H_{3M}^+ &= -\frac{s_{2M}}{c_M} \phi_2^+ + \frac{s_2}{c_M} \phi_{2M}^+, \\ H_{3M}^0 &= \imath \left(-\frac{s_{2M}}{c_M} \phi_2^{0\imath} + \frac{s_2}{c_M} \phi_{2M}^{0\imath} \right), \\ H_1^0 &= \phi_2^{0r}, \quad H_{1M}^0 = \phi_{2M}^{0r}, \\ H_1^{0'} &= \frac{1}{\sqrt{3}} \left(\sqrt{2}\chi^{0r} + \xi^0 \right) \quad (\text{A22})\end{aligned}$$

with phase conventions $H_5^{--} = (H_5^{++})^*$, $H_5^- = -(H_5^+)^*$, $H_3^- = -(H_3^+)^*$, $H_{3M}^- = -(H_{3M}^+)^*$, $H_3^0 = -(H_3^0)^*$ and $H_{3M}^0 = -(H_{3M}^0)^*$. The masses of these physical scalars can easily be obtained from eq. (A15). Since, the potential preserves the $SU(2)_D$ custodial symmetry, members of

the physical scalar multiplets have degenerate masses. These masses are

$$\begin{aligned}m_5^2 &= 3(\lambda_5 c_M^2 + \lambda_8 s_M^2) v^2, \\ m_3^2 &= \lambda_5 v^2, \quad m_{3M}^2 = \lambda_5 (1 + c_M^2) v^2, \quad (\text{A23})\end{aligned}$$

In general, the H_1^0 , H_{1M}^0 and $H_1^{0'}$ can mix according to the mass-squared matrix

$$\mathcal{M}_{\text{singlets}}^2 = v^2 \times \begin{pmatrix} 8s_2^2(\lambda_1 + \lambda_4) & 8s_2 s_{2M} \lambda_4 & 2\sqrt{6} s_2 s_M \lambda_4 \\ 8s_2 s_{2M} \lambda_4 & 8s_{2M}^2(\lambda_2 + \lambda_4) & 2\sqrt{6} s_{2M} s_M \lambda_4 \\ 2\sqrt{6} s_2 s_M \lambda_4 & 2\sqrt{6} s_{2M} s_M \lambda_4 & 3s_M^2(\lambda_3 + \lambda_4) \end{pmatrix} \quad (\text{A24})$$

Hence, the generic mass eigenstates are given by Eq. (24). It should be noted that in the limit $\lambda_4 \rightarrow 0$ the off-diagonal elements in the matrix above vanish. Also note that, in general, we have six parameters in the physical scalar potential and we *can* have six independent physical scalar masses. Thus, given the masses of the physical scalar states the parameters (these include quadratic coupling parameters, λ_4 , λ_5 , λ_8) in the potential can be uniquely determined and vice versa.

TABLE VI. Yukawa couplings with SM quarks and mirror-quarks in the EW ν_R model. The Yukawa couplings involving *charged* SM (and mirror) leptons can be obtained by replacing up-type SM (and mirror) quarks by left-handed (and right-handed) neutrinos and down-type SM (and mirror) quarks by the charged SM (and mirror) leptons in this table.

SM Quarks	Mirror Quarks
$g_{H_1^0 q \bar{q}} \quad -i \frac{m_q g}{2 M_W s_2} \dots (q = t, b)$	$g_{H_{1M}^0 q^M \bar{q}^M} \quad -i \frac{m_q^M g}{2 M_W s_{2M}}$
$g_{H_3^0 t \bar{t}} \quad i \frac{m_t g s_M}{2 M_W c_M} \gamma_5$	$g_{H_{3M}^0 u_i^M \bar{u}_i^M} \quad -i \frac{m_{u_i^M} g s_M}{2 M_W c_M} \gamma_5$
$g_{H_3^0 b \bar{b}} \quad -i \frac{m_b g s_M}{2 M_W c_M} \gamma_5$	$g_{H_{3M}^0 d_i^M \bar{d}_i^M} \quad i \frac{m_{d_i^M} g s_M}{2 M_W c_M} \gamma_5$
$g_{H_3^- t \bar{b}} \quad i \frac{g s_M}{2\sqrt{2} M_W c_M} [m_t(1 + \gamma_5) - m_b(1 - \gamma_5)]$	$g_{H_{3M}^- u_i^M \bar{b}_i^M} \quad i \frac{g s_M}{2\sqrt{2} M_W c_M} [m_{u_i^M}(1 - \gamma_5) - m_{d_i^M}(1 + \gamma_5)]$
$g_{H_{3M}^0 t \bar{t}} \quad -i \frac{m_t g s_{2M}}{2 M_W s_2} \gamma_5$	$g_{H_{3M}^0 u_i^M \bar{u}_i^M} \quad -i \frac{m_{u_i^M} g s_2}{2 M_W s_{2M}} \gamma_5$
$g_{H_{3M}^0 b \bar{b}} \quad i \frac{m_b g s_{2M}}{2 M_W s_2} \gamma_5$	$g_{H_{3M}^0 d_i^M \bar{d}_i^M} \quad i \frac{m_{d_i^M} g s_2}{2 M_W s_{2M}} \gamma_5$
$g_{H_{3M}^- t \bar{b}} \quad i \frac{g s_{2M}}{2\sqrt{2} M_W s_2 c_M} [m_t(1 + \gamma_5) - m_b(1 - \gamma_5)]$	$g_{H_{3M}^- u_i^M \bar{d}_i^M} \quad i \frac{g s_2}{2\sqrt{2} M_W s_{2M} c_M} [m_{u_i^M}(1 - \gamma_5) - m_{d_i^M}(1 + \gamma_5)]$
$g_{H_1^0 l \bar{l}} \quad -i \frac{m_l g}{2 M_W s_2} \dots (l = \tau, \mu, e)$	$g_{H_{1M}^0 l^M \bar{l}^M} \quad -i \frac{m_l^M g}{2 M_W s_{2M}}$
$g_{H_3^0 l \bar{l}} \quad -i \frac{m_l g s_M}{2 M_W c_M} \gamma_5$	$g_{H_{3M}^0 l_i^M \bar{l}_i^M} \quad i \frac{m_{l_i^M} g s_M}{2 M_W c_M} \gamma_5$
$g_{H_3^- \nu_L \bar{l}} \quad -i \frac{g m_l s_M}{2\sqrt{2} M_W c_M} (1 - \gamma_5)$	$g_{H_{3M}^- \nu_{Ri} \bar{l}_i^M} \quad -i \frac{g m_{l_i^M} s_M}{2\sqrt{2} M_W c_M} (1 + \gamma_5)$
$g_{H_{3M}^0 l \bar{l}} \quad i \frac{m_l g s_{2M}}{2 M_W s_2} \gamma_5$	$g_{H_{3M}^0 l_i^M \bar{l}_i^M} \quad i \frac{m_{l_i^M} g s_2}{2 M_W s_{2M}} \gamma_5$
$g_{H_{3M}^- \nu_L \bar{l}} \quad -i \frac{g m_l s_{2M}}{2\sqrt{2} M_W s_2 c_M} (1 - \gamma_5)$	$g_{H_{3M}^- \nu_{Ri} \bar{l}_i^M} \quad -i \frac{g m_{l_i^M} s_2}{2\sqrt{2} M_W s_{2M} c_M} (1 + \gamma_5)$

TABLE VII. $S_1 S_2 V$ type couplings (V is a vector gauge boson and S_1, S_2 are Higgs/ Goldstone bosons), which contribute to Oblique Corrections. Common factor: $ig(p - p')^\mu$, where $p(p')$ is the *incoming* momentum of the $S_1(S_2)$.

$g_{H_5^0 H_5^- W^+}$	$-\frac{\sqrt{3}}{2}$	$g_{H_5^{++} H_5^{--} Z}$	$-\frac{(1 - 2s_W^2)}{c_W}$
$g_{H_5^+ H_5^{--} W^+}$	$-\frac{1}{\sqrt{2}}$	$g_{H_5^+ H_5^- Z}$	$\frac{(1 - 2s_W^2)}{2c_W}$
$g_{H_3^0 H_3^- W^+}$	$-\frac{1}{2}s_M^2$	$g_{H_3^+ H_3^- Z}$	$\frac{(1 - 2s_W^2)}{2c_W}$
$g_{H_{3M}^0 H_{3M}^- W^+}$	$\frac{1}{2}$	$g_{H_{3M}^+ H_{3M}^- Z}$	$\frac{(1 - 2s_W^2)}{2c_W}$
$g_{H_3^+ H_5^{--} W^+}$	$-\frac{1}{\sqrt{2}}c_M$	$g_{H_3^+ H_5^- Z}$	$-\frac{1}{2c_W}c_M$
$g_{H_3^0 H_5^- W^+}$	$-\frac{1}{2}c_M$	$g_{H_3^0 H_3^0 Z}$	$\frac{1}{\sqrt{3}}\frac{c_M}{c_W}$
$g_{H_5^0 H_3^- W^+}$	$-\frac{1}{2\sqrt{3}}c_M$	$g_{G_3^+ G_3^- Z}$	$\frac{(1 - 2s_W^2)}{2c_W}$
$g_{G_3^0 G_3^- W^+}$	$-\frac{1}{2}$	$g_{G_3^0 H_5^0 Z}$	$\frac{1}{\sqrt{3}}\frac{s_M}{c_W}$
$g_{G_3^+ H_5^{--} W^+}$	$-\frac{1}{\sqrt{2}}s_M$	$g_{G_3^+ H_5^- Z}$	$-\frac{1}{2c_W}s_M$
$g_{G_3^+ H_5^{--} W^+}$	$-\frac{1}{\sqrt{2}}s_M$	$g_{H_1^0 G_3^0 Z}$	$\frac{s_2}{c_W}$
$g_{G_3^0 H_5^- W^+}$	$-\frac{1}{2}s_M$	$g_{H_{1M}^0 G_3^0 Z}$	$\frac{s_{2M}}{c_W}$
$g_{H_5^0 G_3^- W^+}$	$\frac{1}{2\sqrt{3}}s_M$	$g_{H_1^0 G_3^0 Z}$	$\sqrt{\frac{2}{3}}\frac{s_M}{c_W}$
$g_{H_5^0 G_3^- W^+}$	$\frac{1}{2\sqrt{3}}s_M$	$g_{H_1^0 H_3^0 Z}$	$-\frac{s_2 s_M}{2c_M c_W}$
$g_{H_1^0 G_3^- W^+}$	$\frac{1}{2}s_2$	$g_{H_{1M}^0 H_3^0 Z}$	$-\frac{s_{2M} s_M}{2c_M c_W}$
$g_{H_{1M}^0 G_3^- W^+}$	$\frac{1}{2}s_{2M}$	$g_{H_1^0 H_3^0 Z}$	$\sqrt{\frac{2}{3}}\frac{c_M}{c_W}$
$g_{H_1^0 G_3^- W^+}$	$\sqrt{\frac{2}{3}}s_M$	$g_{H_5^+ H_5^- \gamma}$	sw
$g_{H_1^0 H_3^- W^+}$	$-\frac{s_2 s_M}{2c_M}$	$g_{H_5^{++} H_5^{--} \gamma}$	$-2sw$
$g_{H_{1M}^0 H_3^- W^+}$	$-\frac{s_{2M} s_M}{2c_M}$	$g_{H_3^+ H_3^- \gamma}$	sw
$g_{H_1^0 H_3^- W^+}$	$\sqrt{\frac{2}{3}}c_M$	$g_{H_{3M}^+ H_{3M}^- \gamma}$	sw
$g_{H_1^0 H_{3M}^- W^+}$	$-\frac{s_{2M}}{2c_M}$	$g_{G_3^+ G_3^- \gamma}$	sw
$g_{H_{1M}^0 H_{3M}^- W^+}$	$\frac{s_2}{2c_M}$	$g_{H_1^0 H_{3M}^0 Z}$	$\frac{s_{2M}}{2c_M}$
		$g_{H_{1M}^0 H_{3M}^0 Z}$	$-\frac{s_2}{2c_M}$

TABLE VIII. SV_1V_2 type couplings (V_1 and V_2' are vector gauge bosons and S is a Higgs boson), which contribute to Oblique Corrections. Common factor: $igM_W g^{\mu\nu}$

$g_{H_5^0 W^+ W^-}$	$\frac{s_M}{\sqrt{3}}$	$g_{H_5^0 Z Z}$	$-\frac{2}{\sqrt{3}} \frac{s_M}{c_W^2}$
$g_{H_5^{++} W^- W^-}$	$\sqrt{2} s_M$	$g_{H_5^+ W^- Z}$	$-\frac{s_M}{c_W}$
$g_{H_1^0 W^+ W^-}$	s_2	$g_{H_1^0 Z Z}$	$\frac{s_2}{c_W^2}$
$g_{H_{1M}^0 W^+ W^-}$	s_{2M}	$g_{H_{1M}^0 Z Z}$	$\frac{s_{2M}}{c_W^2}$
$g_{H_1^{0'} W^+ W^-}$	$\frac{2\sqrt{2}}{\sqrt{3}} s_M$	$g_{H_1^{0'} Z Z}$	$\frac{2\sqrt{2}}{\sqrt{3}} \frac{s_M}{c_W^2}$

TABLE IX. $H_1 H_2 V_1 V_2$ type couplings, which contribute to Oblique Corrections. Common factor: $ig^2 g^{\mu\nu}$

$g_{H_5^0 H_5^0 W^+ W^-}$	$\frac{5}{3}$	$g_{H_5^0 H_5^0 Z Z}$	$\frac{2}{3c_W^2}$
$g_{H_5^+ H_5^- W^+ W^-}$	$-\frac{3}{2}$	$g_{H_5^+ H_5^- Z Z}$	$-\frac{(c_W^4 + s_W^4)}{c_W^2}$
$g_{H_5^{++} H_5^{--} W^+ W^-}$	1	$g_{H_5^{++} H_5^{--} Z Z}$	$2 \frac{(1 - 2s_W^2)^2}{c_W^2}$
$g_{H_3^0 H_3^0 W^+ W^-}$	$-\frac{(1 + c_M^2)}{2}$	$g_{H_3^0 H_3^0 Z Z}$	$-\frac{1}{2c_W^2} (1 + 3c_M^2)$
$g_{H_3^+ H_3^- W^+ W^-}$	$-\left(\frac{1}{2} + c_M^2\right)$	$g_{H_3^+ H_3^- Z Z}$	$-\left[\frac{s_M^2}{2} \frac{(1 - s_W^2)^2}{c_W^2} + c_M^2 \frac{(c_W^4 + s_W^4)}{c_W^2} \right]$
$g_{H_{3M}^0 H_{3M}^0 W^+ W^-}$	$-\frac{1}{2}$	$g_{H_{3M}^0 H_{3M}^0 Z Z}$	$\frac{1}{2c_W^2}$
$g_{H_{3M}^+ H_{3M}^- W^+ W^-}$	$-\frac{1}{2}$	$g_{H_{3M}^+ H_{3M}^- Z Z}$	$-\frac{(1 - 2s_W^2)^2}{2c_W^2}$
$g_{G_3^0 G_3^0 W^+ W^-}$	$-\frac{(1 + s_M^2)}{2}$	$g_{G_3^0 G_3^0 Z Z}$	$-\frac{1}{2c_W^2} (1 + 3s_M^2)$
$g_{G_3^+ G_3^- W^+ W^-}$	$-\left(\frac{1}{2} + s_M^2\right)$	$g_{G_3^+ G_3^- Z Z}$	$-\left[\frac{c_M^2}{2} \frac{(1 - s_W^2)^2}{c_W^2} + s_M^2 \frac{(c_W^4 + s_W^4)}{c_W^2} \right]$
$g_{H_1^0 H_1^0 W^+ W^-}$	$\frac{1}{2}$	$g_{H_1^0 H_1^0 Z Z}$	$\frac{1}{2c_W^2}$
$g_{H_{1M}^0 H_{1M}^0 W^+ W^-}$	$\frac{1}{2}$	$g_{H_{1M}^0 H_{1M}^0 Z Z}$	$\frac{1}{2c_W^2}$
$g_{H_1^{0'} H_1^{0'} W^+ W^-}$	$\frac{4}{3}$	$g_{H_1^{0'} H_1^{0'} Z Z}$	$\frac{4}{3c_W^2}$
$g_{H_5^+ H_5^- \gamma \gamma}$	$-2s_W^2$	$g_{H_5^+ H_5^- Z \gamma}$	$-\frac{s_W}{c_W} (1 - 2s_W^2)$
$g_{H_5^{++} H_5^{--} \gamma \gamma}$	$8s_W^2$	$g_{H_5^{++} H_5^{--} Z \gamma}$	$4 \frac{s_W}{c_W} (1 - 2s_W^2)$
$g_{H_3^+ H_3^- \gamma \gamma}$	$-2s_W^2$	$g_{H_3^+ H_3^- Z \gamma}$	$-\frac{s_W}{c_W} (1 - 2s_W^2)$
$g_{H_{3M}^+ H_{3M}^- \gamma \gamma}$	$-2s_W^2$	$g_{H_{3M}^+ H_{3M}^- Z \gamma}$	$-\frac{s_W}{c_W} (1 - 2s_W^2)$
$g_{G_3^+ G_3^- \gamma \gamma}$	$-2s_W^2$	$g_{G_3^+ G_3^- Z \gamma}$	$-\frac{s_W}{c_W} (1 - 2s_W^2)$

TABLE X. $H_1 H_2 V_1 V_2$ type couplings, which *do not* contribute to Oblique Corrections. Common factor: $ig^2 g^{\mu\nu}$

$g_{H_1^{0'} H_5^0 W^+ W^-}$	$\frac{\sqrt{2}}{3}$	$g_{H_1^{0'} H_5^0 Z Z}$	$-\frac{2\sqrt{2}}{3c_W^2}$
$g_{H_3^+ H_5^- W^+ W^-}$	$-\frac{c_M}{2}$	$g_{H_3^+ H_5^- Z Z}$	$c_M \frac{(1 - 2s_W^2)}{c_W^2}$
$g_{H_3^0 G_3^0 W^+ W^-}$	$-\frac{c_M s_M}{2}$	$g_{H_3^0 G_3^0 Z Z}$	$-\frac{3}{2} \frac{c_M s_M}{c_W^2}$
$g_{H_3^+ G_3^- W^+ W^-}$	$-c_M s_M$	$g_{H_3^+ G_3^- Z Z}$	$-\frac{c_M s_M}{2c_W^2}$
$g_{H_5^+ G_3^- W^+ W^-}$	$-\frac{s_M}{2}$	$g_{H_5^+ G_3^- Z Z}$	$s_M \frac{(1 - 2s_W^2)}{c_W^2}$
		$g_{H_3^+ H_5^- Z \gamma}$	$c_M \frac{s_W}{c_W}$

Appendix B: Partial decay widths of neutral Higgs

In this section we will discuss various production and decay channels relevant for studying properties of \tilde{H} , \tilde{H}' and \tilde{H}'' [8]. Out of these $H^0 \rightarrow \gamma\gamma$, gg - type decays (and also the Higgs boson production through $gg \rightarrow H$) have only one loop contributions at the leading order (LO) and decays like $H^0 \rightarrow WW$, ZZ , $f\bar{f}$ can take place through tree level interactions. We show calculation of the decay width $\Gamma(H \rightarrow \gamma\gamma)$ up to LO in QCD. We will show how all the other relevant decay widths can be calculated easily from the corresponding SM values modified by a multiplicative factor. We calculate these widths in $EW\nu_R$ model from the SM values given in [8].

1. $H \rightarrow gg$

The decay of a custodial singlet Higgs boson to two gluons proceeds through one-loops at LO. Unlike $H^0 \rightarrow \gamma\gamma$ channel this channel does not give a ‘clean’ signal at a hadron collider like LHC due to large QCD background. But gluon-gluon fusion channel ($gg \rightarrow H$) is the most dominant production channel for a neutral Higgs and hence, Hgg coupling becomes important while studying $\mu(H^0\text{-decay})$ for various decay channels. The production cross section of $gg \rightarrow H^0$ is related to the width of $H^0 \rightarrow gg$ by

$$\sigma(gg \rightarrow H^0) \propto \Gamma(H^0 \rightarrow gg), \quad (\text{B1})$$

where the constant of proportionality includes phase space integrals and the mass of H^0 (refer Eq. (2.30) in [9]). Therefore, for a given mass of Higgs

$$\frac{\sigma_{EW\nu_R}(gg \rightarrow H^0)}{\sigma_{SM}(gg \rightarrow H^0)} = \frac{\Gamma_{EW\nu_R}(H^0 \rightarrow gg)}{\Gamma_{SM}(H^0 \rightarrow gg)}. \quad (\text{B2})$$

Hence, to calculate signal strengths $\mu(H\text{-decay})$, we use $\Gamma(H^0 \rightarrow gg)$ instead of $\Gamma(H^0 \rightarrow \gamma\gamma)$, since we are only interested in the ratios of production cross-sections.

Consider a general scalar mass-eigenstate H that is also a CP-even state in some model of BSM Physics. The relevant part of the interaction Lagrangian is [9]

$$\begin{aligned} \mathcal{L}_{int} = & \frac{-m_f}{v_{H^0}} \bar{\psi}\psi H^0 + g M_W \lambda_W W_\mu^+ W^{\mu-} H^0 \\ & + \frac{g \lambda_S}{M_W} S^+ S^- H^0, \end{aligned} \quad (\text{B3})$$

where v_{H^0} is the vacuum expectation value of H^0 , $v = 2M_W/g \sim \sqrt{\sum_{\text{all } H^0\text{'s}} v_{H^0}^2}$, ψ is a fermion of mass m_f ,

S^\pm is a charged BSM scalar. For SM $\lambda_W = 1/\sqrt{2}$, $\lambda_S = 0$. For a general (CP-even) Higgs boson H^0 that couples to the SM quarks with Yukawa coupling in the equation above, the decay width of $H^0 \rightarrow gg$ is given by

$$\Gamma(H^0 \rightarrow gg) = \frac{\alpha_S^2 g^2 m_{H^0}^3}{128\pi^3 M_W^2} \left| \sum_i \frac{1}{2 v_{H^0}/v} F_{1/2}(\tau_i) \right|^2, \quad (\text{B4})$$

where, for a loop of quark having mass m_i , $\tau_i = 4m_i^2/m_{H^0}$ [9], and $F_{1/2}(\tau)$ is given by

$$F_{1/2}(\tau) = -2\tau[1 + (1-\tau)f(\tau)]. \quad (\text{B5})$$

and

$$\begin{aligned} f(\tau) &= [\sin^{-1}(1/\sqrt{\tau})]^2, & \text{if } \tau \geq 1, \\ &= \frac{1}{4} [\text{Log}(\eta_+/\eta_-) - i\pi]^2, & \text{if } \tau < 1; \end{aligned} \quad (\text{B6})$$

where

$$\eta_\pm \equiv (1 \pm \sqrt{1-\tau}). \quad (\text{B7})$$

In [8] the width for $H^0 \rightarrow gg$ in SM is calculated up to the NLO QCD calculations. We calculate $\Gamma(\tilde{H} \rightarrow gg)$ in the $EW\nu_R$ model using these SM values. Using Eq. (24) and Table VI this decay width can be given by

$$\begin{aligned} \Gamma^{EW\nu_R}(\tilde{H} \rightarrow gg) &= \Gamma^{SM}(H_{SM}^0 \rightarrow gg) \times \frac{1}{|F_{1/2}(\tau_{top})|^2} \\ &\times \left| \frac{a_{\tilde{H},1}}{s_2} F_{1/2}(\tau_{top}) + \frac{a_{\tilde{H},1M}}{s_{2M}} \sum_i F_{1/2}(\tau_{MF_i}) \right|^2 \end{aligned} \quad (\text{B8})$$

where \tilde{H} denotes \tilde{H} , \tilde{H}' and \tilde{H}'' ; \sum_i is over all the mirror quarks; $\tau_{MF_i} = 4m_{MF_i}^2/m_{H^0}^2$. $a_{\tilde{H},1}$ and $a_{\tilde{H},1M}$ are elements of the square matrix in Eq (24) - they are coefficients of H_1^0 and H_{1M}^0 in \tilde{H} respectively.

2. $H^0 \rightarrow \gamma\gamma$

For a custodial singlet Higgs boson decay to two photons also proceeds through one-loops at LO. It is a ‘clean’ channel due to the absence of large QCD background. Therefore, in the study of 126 GeV Higgs boson, decay to diphoton is an important channel at CMS and ATLAS [21, 23].

For a general Higgs mass eigenstate H^0 having couplings as given in Eq (B3) the decay width of $H^0 \rightarrow \gamma\gamma$ is given by [9]:

$$\Gamma(H^0 \rightarrow \gamma\gamma) = \frac{\alpha^2 g^2}{1024 \pi^3} \frac{m_{H^0}^3}{M_W^2} \left| \sum_i N_{ci} Q_i^2 F_s(\tau_i) \right|^2. \quad (\text{B9})$$

Here \sum_i is performed over all the particles of spin- s which contribute to $H^0 \rightarrow \gamma\gamma$, $s = \text{spin-0, spin-1/2, and spin-1}$ is the spin of i^{th} particle, Q_i is the electric charge in units of e , and

$$\begin{aligned} F_1(\tau) &= \lambda_W \tau [3 + (4 - 3\tau)f(\tau)], \\ F_{1/2}(\tau) &= -2\tau[1 + (1 - \tau)f(\tau)], \\ F_0(\tau) &= 2\lambda_S [1 - \tau f(\tau)], \end{aligned} \quad (\text{B10})$$

with $\tau = 4m_i^2/m_{H^0}^2$ and $f(\tau)$ is given by Eq (B6).

Considering the contribution from W^\pm loop, the charged fermion loops in SM (all except the top quark loop are negligible) and setting $v_{H^0} = v$ gives the $H_{SM}^0 \rightarrow \gamma\gamma$ decay width. Note that $F_1(\tau)$ includes contributions from only the transverse polarization of W-boson; the contribution from Goldstone boson must be added separately using $F_0(\tau_W)$.²

Based on Eq (B9) we define partial amplitude of $H^0 \rightarrow \gamma\gamma$ as

$$\mathcal{A}(H^0 \rightarrow \gamma\gamma) = \sqrt{\frac{\alpha^2 g^2}{1024 \pi^3} \frac{m_{H^0}^3}{M_W^2}} \left(\sum_i N_{ci} Q_i^2 F_s(\tau_i) \right). \quad (\text{B11})$$

Then, in the $\text{EW}\nu_R$ model, we see from Eq (24) that

$$\begin{aligned} \Gamma^{\text{EW}\nu_R}(\tilde{H} \rightarrow \gamma\gamma) &= \left| a_{\tilde{H},1} \mathcal{A}^{\text{EW}\nu_R}(H_1^0 \rightarrow \gamma\gamma) \right. \\ &+ a_{\tilde{H},1M} \mathcal{A}^{\text{EW}\nu_R}(H_{1M}^0 \rightarrow \gamma\gamma) \\ &+ \left. a_{\tilde{H},1'} \mathcal{A}^{\text{EW}\nu_R}(H_{1'}^0 \rightarrow \gamma\gamma) \right|^2, \end{aligned} \quad (\text{B12})$$

where $a_{\tilde{H},i}$ with $(i = 1, 1M, 1')$ are the coefficients of H_1^0 , H_{1M}^0 and $H_{1'}^0$ in \tilde{H} mass eigenstate, respectively; these are the elements in the \tilde{H} -row of the mixing matrix in Eq (24). To calculate $\mathcal{A}^{\text{EW}\nu_R}(H_1^0 \rightarrow \gamma\gamma)$, in addition to the W^\pm , G_3^\pm and top-loop contributions we have to also consider one loop contributions involving H_3^\pm , H_{3M}^\pm , H_5^\pm and $H_5^{\pm\pm}$, whereas for $\mathcal{A}^{\text{EW}\nu_R}(H_{1M}^0 \rightarrow \gamma\gamma)$ we need to consider the W^\pm , G_3^\pm loops, the loops with the charged mirror fermion and the loops with H_3^\pm , H_{3M}^\pm , H_5^\pm and $H_5^{\pm\pm}$. Various Feynman rules necessary for these calculations can be read from Tables VI-X and the three point scalar Feynman rules can be obtained from [Scalar potential equation].

In Eq.[eqn for masses of multiplet scalars] all the members of a scalar custodial multiplet are degenerate, e.g.

H_3^0 and H_3^+ have same masses and so on. But once custodial symmetry is broken at the loop level, different custodial multiplet members can have different masses. This mass splitting can also be due to some custodial symmetry-breaking terms in the Lagrangian (not given explicitly in this paper). In that case, the partial width of $\tilde{H} \rightarrow \gamma\gamma$ depends on the following variable parameters in $\text{EW}\nu_R$ models are:

- Masses of H_3^\pm , H_{3M}^\pm , H_5^\pm and $H_5^{\pm\pm}$;
- s_2 , s_{2M} , s_M ;
- Masses of charged mirror leptons and mirror quarks;
- Scalar self-couplings: λ_1 , λ_2 , λ_3 , λ_4 , λ_5 , λ_8 ;
- Elements of 3×3 mixing matrix in Eq (24).

Note that all of these parameters are not completely independent, e.g. once we fix s_2 , s_{2M} , then s_M is automatically fixed; scalar self-couplings and mixing matrix elements must vary so as to give at least one scalar mass eigenstate at 126 GeV, etc.

3. Tree level decays of \tilde{H}

Tree level decay channels of a neutral (CP-even) Higgs include decays to two fermions and to WW , ZZ . In this subsection first we show how the decay widths of these decays in the $\text{EW}\nu_R$ model are related to the widths in SM. Although at the LO these decays have only the tree level contributions, NLO QCD+EW corrections become significant at about 5% accuracy for [8]. Because the decay widths of these channels at tree level in the $\text{EW}\nu_R$ model and in SM are related by a multiplicative factor as described below, by using SM decay widths to calculate the decay widths in $\text{EW}\nu_R$ model these NLO contributions will be automatically included in our results. For vertices involving mirror fermions the QCD+EW corrections are different from the corrections for SM quarks (in SM non-negligible QCD corrections only come from top quark). Because mirror quark masses are of the same order as the top quark, for $\sim 5\%$ accuracy the NLO corrections due to mirror quarks can be assumed to have the same magnitude as those due to the top quark. The different tree level couplings in $\text{EW}\nu_R$ model can be found in Tables VI, VIII, and Eq.[eqn. with relevant Lagrangian terms]). Note that the predictions for μ of various decay channels in the

² The formulas given above in Eq (B3), Eq (B10) are a bit different from Eqs.(2.15), (2.17) in [9]. We try to give formulas for a general BSM model (e.g. using a general v_{H^0} , λ_W and λ_S)

EW ν_R model are stated up to 5% accuracy, because Yukawa couplings of H_{1M}^0 with the mirror fermions can be large and at these large values extra QCD corrections can be dominant and reduce the accuracy to $\sim 5\%$.

$\tilde{H} \rightarrow \mathbf{WW}, \mathbf{ZZ}$:

The $H_1^0 VV$, $H_{1M}^0 VV$ and $H_1^{0'} VV$ couplings ($V = W^\pm, Z$) in EW ν_R model are suppressed by $s_2 = v_2/v$, $s_{2M} = v_{2M}/v$ and $s_M = 2\sqrt{2}v_M/v$ respectively, as compared to $H_{SM}^0 VV$ couplings in SM. Hence, using Eq (24) the decay widths for custodial singlet Higgs mass eigenstates \tilde{H} are given by

$$\Gamma^{EW\nu_R}(\tilde{H} \rightarrow WW, ZZ) = \Gamma^{SM}(H_{SM}^0 \rightarrow WW, ZZ) \times |a_{\tilde{H},1} s_2 + a_{\tilde{H},1M} s_{2M} + a_{\tilde{H},1'} \frac{2\sqrt{2}}{\sqrt{3}} s_M|^2. \quad (\text{B13})$$

$\tilde{H} \rightarrow \mathbf{f}\bar{\mathbf{f}}$:

The decays of $\tilde{H}, \tilde{H}', \tilde{H}''$ to two fermions take place through the tree level Yukawa couplings at LO, when mass of the decaying scalar is at least twice as much as mass of the fermions. It can be seen from Table VI that the Yukawa couplings of charged SM fermions with H_1^0 and H_{1M}^0 are enhanced by factors $1/s_2$ and $1/s_{2M}$ respectively as compared to the corresponding couplings with H_{SM}^0 in SM. Also, $H_1^{0'}$ does not couple to particle-antiparticle pairs of charged fermions. Hence, the decay widths to SM fermions can be calculated from corresponding SM decay widths given in [8] and using Eq (24). Decay widths calculated in this way also include NLO QCD corrections that are taken into account in [8]. The partial widths of decays to SM fermions are given in terms of corresponding widths in SM by

$$\Gamma^{EW\nu_R}(\tilde{H} \rightarrow f \bar{f}) = \Gamma^{SM}(H^0 \rightarrow f \bar{f}) \times \left| \frac{a_{\tilde{H},1}}{s_2} \right|^2, \quad (\text{B14})$$

On the other hand, the partial widths of decays to two charged mirror fermions need to be calculated explicitly. We calculate these up to LO, i.e. up to $\sim 5\%$ accuracy, since for further accuracy NLO QCD corrections become important. These partial widths are given by

$$\Gamma^{EW\nu_R}(\tilde{H} \rightarrow f^M \bar{f}^M) = \frac{g^2}{32\pi} \frac{m_{f^M}^2}{M_W^2} \frac{a_{\tilde{H},1M}^2}{s_{2M}^2} m_{\tilde{H}} \times \left(1 - \frac{4 m_{f^M}^2}{m_{\tilde{H}}^2} \right)^{3/2}. \quad (\text{B15})$$

Total width of \tilde{H} :

The total widths of a mass eigenstates $\tilde{H}, \tilde{H}', \tilde{H}''$ can be calculated by adding individual partial widths of various decay channels. We consider all the kinematically allowed channels among $W^+W^-, ZZ, \gamma\gamma, gg, b\bar{b}, t\bar{t}, \tau\bar{\tau}, \mu\bar{\mu}, c\bar{c}, l^M \bar{l}^M$ and $q^M \bar{q}^M$.

Appendix C: Amplitude of $H_3 \rightarrow WW/ZZ$

The process such as $H_3^0 \rightarrow WW/ZZ$ in this model only happens at the loop level. At 1 loop, the Feynman diagrams are:

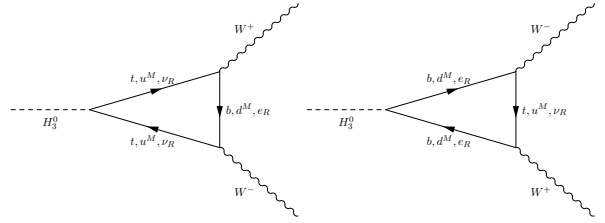


FIG. 20. Feynman diagram of $H_3^0 \rightarrow W^+W^-$. We have three generations of mirror quarks and three generations of mirror leptons

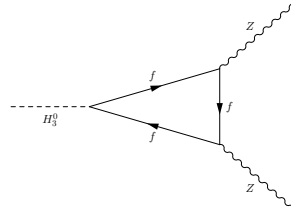


FIG. 21. Feynman diagram of $H_3^0 \rightarrow ZZ$. Here, $f = u_1^M, d_1^M, u_2^M, d_2^M, u_3^M, d_3^M$, and three charged mirror leptons l^M

With the couplings in the table (??), the amplitude can be expressed as [?]:

$$A(H_3^0 \rightarrow VV) = m_u^2 t_M A_u^V - m_d^2 t_M A_d^V \quad (\text{C1})$$

u, d here represent $t, b; u_M^i, d_M^i; \nu_R^j, l_M^j$. Two intermediate function A_u^V, A_d^V are expressed in terms of loop functions, C, F [31]:

- $H_3^0 \rightarrow W^+W^-$

$$A_u^W = \frac{1}{2} [C(m_W^2; m_u^2, m_d^2) + F(m_W^2; m_u^2, m_d^2)]$$

$$A_d^W = \frac{1}{2} [C(m_W^2; m_d^2, m_u^2) + F(m_W^2; m_d^2, m_u^2)]$$

(C2)

- $H_3^0 \rightarrow ZZ$

$$A_f^Z = \left[\frac{(T_3 - Q \sin^2 \theta_W)^2}{\cos^2 \theta_W} + \left(\frac{Q \sin^2 \theta_W}{\cos \theta_W} \right)^2 \right] C(m_Z^2; m_f^2) \\ + \left[\frac{(T_3 - Q \sin^2 \theta_W)^2}{\cos^2 \theta_W} - \left(\frac{Q \sin^2 \theta_W}{\cos \theta_W} \right)^2 \right] F(m_Z^2; m_f^2) \quad (C3)$$

C, F are generally in form of the 't Hooft-Veltman scalar loop integrals [31]. But here, we have top quark and heavy mirror fermions. So, we can use asymptotic forms

in the high mass limit.

$$C(m_V^2; m_u^2, m_d^2) = \int_0^1 dx \int_0^x dy \frac{1}{D} \\ F(m_V^2; m_u^2, m_d^2) = - \int_0^1 dx \int_0^x dy \frac{1}{D} \quad (C4)$$

Where

$$D = m_{H_3^0}^2(1-x)(1-y) + m_V^2(1-x) \\ + m_V^2 y(x-y) - m_u^2(1-y) - m_d^2 y \quad (C5)$$

-
- [1] S. Chatrchyan *et al.* [CMS Collaboration], Phys. Lett. B **716**, 30 (2012) [arXiv:1207.7235 [hep-ex]]; G. Aad *et al.* [ATLAS Collaboration], Phys. Lett. B **716**, 1 (2012) [arXiv:1207.7214 [hep-ex]].
- [2] P. H. Frampton and P. Q. Hung, Mod. Phys. Lett. A **29**, no. 1, 1450006 (2014) [arXiv:1310.3904 [hep-ph]].
- [3] J.C. Pati, A. Salam, Phys. Rev. D **10** (1974) 275; R. N. Mohapatra, J.C. Pati, Phys. Rev. D **11** (1975) 2558; G. Senjanović, R. N. Mohapatra, Phys. Rev. D **12** (1975) 1502; G. Senjanović, Nucl. Phys. B **153** (1979) 334.
- [4] P. Q. Hung, Phys. Lett. B **649**, 275 (2007) [hep-ph/0612004].
- [5] A. Aranda, J. Hernandez-Sanchez and P. Q. Hung, JHEP **0811**, 092 (2008) [arXiv:0809.2791 [hep-ph]].
- [6] V. Hoang, P. Q. Hung and A. S. Kamat, Nucl. Phys. B **877**, 190 (2013) [arXiv:1303.0428 [hep-ph]].
- [7] S. Chatrchyan *et al.* [CMS Collaboration], Phys. Rev. Lett. **110**, 081803 (2013) [arXiv:1212.6639 [hep-ex]].
- [8] SHeinemeyer *et al.* [LHC Higgs Cross Section Working Group Collaboration], arXiv:1307.1347 [hep-ph].
- [9] J. F. Gunion, H. E. Haber, G. L. Kane and S. Dawson, Front. Phys. **80**, 1 (2000).
- [10] A. Djouadi, M. Spira, J. J. van der Bij and P. M. Zerwas, Phys. Lett. B **257**, 187 (1991); A. Djouadi, M. Spira and P. M. Zerwas, Phys. Lett. B **311**, 255 (1993) [hep-ph/9305335]; M. Spira, A. Djouadi, D. Graudenz and P. M. Zerwas, Nucl. Phys. B **453**, 17 (1995) [hep-ph/9504378]; A. Djouadi, M. Spira and P. M. Zerwas, Phys. Lett. B **264**, 440 (1991).
- [11] S. Chatrchyan *et al.* [CMS Collaboration], JHEP **1401**, 096 (2014) [arXiv:1312.1129 [hep-ex]].
- [12] S. Chatrchyan *et al.* [CMS Collaboration], arXiv:1312.5353 [hep-ex].
- [13] S. Chatrchyan *et al.* [CMS Collaboration], Phys. Rev. D **89**, 012003 (2014) [arXiv:1310.3687 [hep-ex]].
- [14] S. Chatrchyan *et al.* [CMS Collaboration], arXiv:1401.5041 [hep-ex].
- [15] S. Chatrchyan *et al.* [CMS Collaboration], arXiv:1401.6527 [hep-ex].
- [16] J. Beringer *et al.* [Particle Data Group Collaboration], Phys. Rev. D **86**, 010001 (2012). We would like to thank Tim Tait for an earlier update.
- [17] M. S. Chanowitz and M. Golden, Phys. Lett. B **165**, 105 (1985).
- [18] Results of SM-like Higgs search at CMS plotted with the help of numerical data provided by Giuseppe Cerati.
- [19] P. Q. Hung, Phys. Lett. B **659**, 585 (2008) [arXiv:0711.0733 [hep-ph]].
- [20] M. Spira, A. Djouadi, D. Graudenz and P. M. Zerwas, Nucl. Phys. B **453**, 17 (1995) [hep-ph/9504378].
- [21] G. Aad *et al.* [ATLAS Collaboration], Phys. Rev. Lett. **113**, no. 17, 171801 (2014) [arXiv:1407.6583 [hep-ex]].
- [22] CMS Collaboration [CMS Collaboration], CMS-PAS-HIG-14-006.
- [23] V. Khachatryan *et al.* [CMS Collaboration], Eur. Phys. J. C **74**, no. 10, 3076 (2014) [arXiv:1407.0558 [hep-ex]].
- [24] S. Heinemeyer *et al.* [LHC Higgs Cross Section Working Group Collaboration], [arXiv:1307.1347 [hep-ph]].
- [25] G. Aad *et al.* [ATLAS Collaboration], [arXiv:1409.6064 [hep-ex]].
- [26] V. Khachatryan *et al.* [CMS Collaboration], [arXiv:1408.3316 [hep-ex]].
- [27] J. F. Gunion, H. E. Haber and C. Kao, Phys. Rev. D **46**, 2907 (1992).
- [28] J. Beringer *et al.* [Particle Data Group Collaboration], Phys. Rev. D **86**, 010001 (2012).
- [29] The ATLAS collaboration, ATLAS-CONF-2013-067, ATLAS-COM-CONF-2013-082.
- [30] S. Chatrchyan *et al.* [CMS Collaboration], Eur. Phys. J. C **73**, 2469 (2013) [arXiv:1304.0213 [hep-ex]].
- [31] G. 't Hooft and M. J. G. Veltman, Nucl. Phys. B **153**, 365 (1979). G. Passarino and M. J. G. Veltman, Nucl. Phys. B **160** (1979) 151.